STD RESEARCH CORPORATION
POST OFFICE BOX "C", ARCADIA, CALIFORNIA 91066-8003
TELEPHONE: (818) 357-2311
FAX: (818) 358-1478

Document Control: Copy 1 of 13

STDR-89-56

TOTAL EXHAUST CONTAINMENT SYSTEM FOR MHD POWER SYSTEMS

FINAL REPORT FOR THE PERIOD
14 SEPTEMBER 1987 – 13 DECEMBER 1989

S.T. Demetriades
C.D. Maxwell
M. Brouillette
G.S. Winckelmans

DECEMBER 1989

STD RESEARCH CORPORATION
POST OFFICE BOX "C"
ARCADIA, CALIFORNIA 91066-8003

PREPARED FOR

U. S. DEPARTMENT OF ENERGY
Pittsburgh Energy Technology Center

UNDER CONTRACT NO. DE-AC22-87PC79677

Accession Number: 4458

Publication Date: Dec 01, 1989

Title: Total Exhaust Containment System For MHD Power Systems

Personal Author: Demetriades, S.T.; Maxwell, C.D.; Brouillette, M. et al.

Corporate Author Or Publisher: STD Research Corp., P.O.Box "C", Arcadia, CA 91066-8003 Report Number: STDR-89-56

Report Prepared for: U.S. Department of Energy, Pittsburgh Energy Technology Center, Pittsburgh, PA

Comments on Document: Final Report for the Period 14 September 1987 - 13 December 1989

Descriptors, Keywords: Exhaust Containment MHD Power TECS MSPS Thermodynamics Heat Transfer Model

Pages: 00044

Cataloged Date: Apr 21, 1993

Contract Number: DE-AC22-87PC79677

Document Type: HC

Number of Copies In Library: 000001

Record ID: 26711

Addendum

to STD Research Corporation Report No. STDR-89-56, "Total Exhaust Containment System For MHD Power Systems," Final Report under Contract DE-AC22-PC79677, December 1989.

NOTICE

TOTAL EXHAUST CONTAINMENT SYSTEM FOR MHD POWER SYSTEMS

Abstract

This effort investigated the feasibility of a revolutionary approach to open-cycle space power system exhaust containment. This approach makes use of state-of-the-art U.S. materials technology and unique designs developed at STD Research Corporation to control the effects of effluents from open-cycle MHD generators operating in space by bagging all the MHD exhaust products in light-weight impermeable containers. Theoretical models for the operation of the Total Exhaust Containment System (TECS) were developed and used to design subscale laboratory simulators. Because of the prohibitive cost of building a complete integrated TECS subscale simulator, the feasibility of the concept was verified by investigating experimentally the performance of each component as sub-assemblies in the high-enthalpy flow facilities at STD Research Corporation. The test program revealed that the materials chosen prior to contract award were adequate for the task, and that the designs for each component fulfilled their role as expected. From those tests and the theoretical scaling laws that were developed in this program, it is estimated that the weight of the TECS system relevant to the STD Research Corporation MHD Space Power System (100 MW_e/500 seconds) is between 5250 and 6250 kg, or between 21 and 25% of the fuel plus oxidant mass, depending on selection of the molecular barrier material. This effluent/reaction control and containment concept can also be applied to other space- or earth-bound open-cycle power generation systems.

On the basis of the theoretical and experimental results presented in the original proposal by STD Research Corporation of 27 January 1987 in response to the DOE/PETC Proposal Request PRDA RA22-87PC90271 and the experimental results obtained after the award of Contract DE-AC22-87PC79677 (start date 14 September 1987) and independently validated and verified by the junior authors of this report by repeating the analyses and experiments during the course of this investigation, it is concluded that the TECS concept proposed by STD Research Corporation exceeds the effluent control requirements for magnetohydrodynamic space power systems set forth on page 34 of the National Research Council Report entitled "Advanced Power Sources for Space Missions, 1989" (Library of Congress Catalog Card No. 88-63907).

TOTAL EXHAUST CONTAINMENT SYSTEM FOR MHD POWER SYSTEMS

Table of Contents

List of Figures

List of Tables

Nomenclature

Roman Letters

A_e	=	Exit Area of MSPS Diffuser
A_e	=	Surface Area of Containment Bag
c_w	=	Heat Capacity of Containment Bag Material
E	=	Internal Energy
E_{th}	=	Thermal Energy of MSPS Effluents
f^*	=	Safety Factor
H	=	Enthalpy
k_w	=	Heat Conductivity of Containment Bag Material
ℓ	=	Distance Separating Momentum Spoiler (MS) from exit of MSPS Diffuser
$\dot{m}$	=	Mass flow rate of MSPS Effluents
M	=	Mass of Containment Bag, Total Mass
$\mathcal{M}$	=	Molecular Mass
n	=	Number of Gas Moles within Containment Bag
p	=	Pressure
p_{max}	=	Burst Pressure of Containment Bag
$\dot{q}_1$	=	Average Radiant Heat Flux Incident on Exterior of Containment Bag
$\dot{Q}_R$	=	Rate of Energy Radiation from Containment Bag to Surroundings
r	=	Radius of Containment Bag
$\mathcal{R}$	=	Universal Gas Constant
R	=	Gas Constant
t	=	Time
T	=	Temperature
t_w	=	Thickness of Containment Bag
V	=	Volume of Containment Bag
x	=	Non-Dimensional Time
y	=	Non-Dimensional Temperature

Greek Letters

γ	=	Ratio of Specific Heats
ϵ	=	Emissivity
η_c	=	Surface Mass Density of Molecular Barrier Material
λ	=	Wavelength
ϖ	=	Ratio of Mass Flow Rate of Gas Effluents to Total Mass Flow Rate
ρ	=	Gas Density
ρ_w	=	Density of Containment Bag Material
σ_B	=	Stefan-Boltzmann Constant
τ_0	=	Characteristic Time of Containment Bag Filling

Subscripts

0	=	Stagnation Conditions of MSPS Effluents

Nomenclature
(Continued)

Subscripts (continued)

1	=	Outer Surface of Containment Bag
2	=	Inner Surface of Containment Bag
3	=	Outer Surface of Filter Bag
4	=	Inner Surface of Filter Bag
f	=	End of Burn
i	=	Start of Burn
gas	=	Gaseous Effluents
tot	=	All Exhaust Effluents
opt	=	Optimum
FB	=	Filter Bag
FCS	=	Force Containment Structure
MB	=	Molecular Barrier
MS	=	Momentum Spoiler
SS	=	Support Structure

CHAPTER I

INTRODUCTION

Open-cycle electric power generation in space or on the surface of the earth offers many important advantages, such as low specific system mass and high efficiency, simplicity, and compactness. At the same time, it presents one possible major disadvantage. It arises from the need to control the open-cycle exhaust and reaction forces in order to ensure that they have no harmful effects on the weapon system and/or platform using that power and their environment.

STD Research Corporation, through an in-house program, has pioneered the development of the technology for open-cycle exhaust and reaction force containment and control in conjunction with its ongoing efforts to develop open-cycle Giant Pulse MHD power generator systems. The advent of new materials and new technologies has made it possible to explore several affordable promising concepts for the control of open-cycle exhaust products and reaction forces and the suppression or elimination of their harmful influences.

STD Research Corporation has performed computations and developed subscale laboratory simulators to demonstrate the feasibility of a Total Exhaust Containment Systems (TECS) concept of wide applicability. It investigated methodologies and conceptual designs for improving the performance and establishing the engineering data base of this concept, with special emphasis on mass reduction and life improvement of the TECS. It calculated and simulated the TECS performance with the appropriate restricted STD Research computer codes and was able to choose the most promising concept. It conducted intensive laboratory tests to determine the most suitable materials for each TECS component and carried out critical experiments in the STD Research high-enthalpy Plasma Flow Facility to validate the calculated results. It is now in position to make recommendations for the rational development of the most promising TECS concept.

1. APPROXIMATE STD/MSPS EXHAUST/TECS INLET DESIGN PARAMETERS

Approximate values of the design data, state points, and other parameters for a typical STD MHD Space Power System (STD/MSPS) relevant to and required for a typical TECS conceptual design exercise are given in Table I.

The composition of a typical STD/MSPS exhaust as well as the composition of the effluents after they have been cooled to a typical condition that would prevail in the containment vessel are listed in the Appendix.

TABLE I

Approximate STD/MSPS TECS Design Parameters

Electrical Power Output	100 MW
Specific Energy Conversion	2 MJ/kg
Duration of Bursts	500 sec
Flow rate	50 Kg/sec
Total Fuel, seed and oxidizer mass	25,000 kg
Thrust	75,530 newtons
Aluminum Oxide (Al_2O_3) in exhaust	10,095 kg
Molecular Weight Al_2O_3	102 kg/(kg-mole)
Gases in exhaust	14,905 kg
Average Molecular Weight of gases	31.83 kg/(kg-mole)
MHD Channel Exit Static Temperature	3231 K
MHD Channel Exit Stagnation Temperature	3370 K
" " " " Enthalpy	8.2 MJ/kg
" " " " Pressure	0.7 atm
" " " Static Pressure	0.4 atm
Average Molecular Weight Exhaust Products	44.08 kg/(kg-mole)
Channel Exit Mass Percentage of Al_2O_3 (liquid)	40.38%
" " Mole " " " "	17.46%
" " Total No. of kg moles Al_2O_3	98.97 kg-moles
" " " " " " " various gases	468.3 kg-moles

Profile Average Quantities	MHD Generator Exit	Diffuser and/or Heat Exchanger Inlet (shocked) /Diffuser Exit	Exit
Pressure (Atm)	0.3854	0.6314	0.27
Temperature (K)	3231	3366	900
Velocity (m/sec)	954.6	657.1/116	59
Mach No.	1.269	0.79/0.14	0.15
c_p/c_v	1.092	1.0924	1.0908
Static Enthalpy (MJ/kg)	7.66	7.94	1.57
Stagn. "	8.15	8.15/7.95	1.57
Area (cm^2)	7121	$7923/4.4\times10^4$	$4/4\times10^4$
Density (kg/m^3)	0.07530	0.09796	0.197
Dynamic Pressure ($newt/m^2$)	3.43×10^4	2.1×10^4	343

2. DESCRIPTION OF THE TECS CONCEPT

The mass, momentum and energy of the effluents exhausting from a typical high-energy open-cycle power system are difficult to contain because they usually emerge from the power generation device in a highly concentrated, fast and energetic stream. Therefore, an effective total exhaust containment system must first diffuse these concentrated mass, momentum and energy fluxes before capturing the effluents. The STD TECS concept fulfills these requirements by integration of carefully engineered components, each of which has a well-defined function.

Fig. 1 is a schematic of the TECS concept as applied to the STD/MSPS. Basically, the TECS consists of three main components or subsystems:

1. The momentum spoiler/energy diffuser (MS).
2. The filter bag (FB).
3. The molecular barrier (MB) with its associated force (*i.e.*, pressure) containment structure.

The function of the momentum spoiler/energy diffuser (MS) is to take the highly concentrated flux of hot exhaust gases as they emerge either directly from the MHD channel or the MHD diffuser or the heat exchanger or any other fast, energetic gas source and to diffuse, spread out and spoil their concentrated momentum and energy. This is done by spreading out the exhaust jet and diffusing and absorbing its momentum and energy by means of a porous, ablating structure of appropriate design. Typically — and this is only by way of illustration — if the MHD exhaust jet at the inlet of the MS is one square unit in cross-sectional area with a dynamic pressure of one unit, it emerges from the MS with something of the order of 10 or more square units in surface area and 0.1 units or less of dynamic pressure.

This is accomplished using specially treated commercial lightweight materials to construct the spoiler structure. Thus, the functions of the MS are:

1. To stop the energetic exhaust jet and transmit most of its reaction forces back to the MSPS support structure so that there is little or no net reaction force from the assembly of the MSPS plus the MS.
2. To diffuse, redistribute, and absorb the energy and momentum of the incident jet in such a manner that no hot spots or high-momentum spots can develop to burn through or puncture the encompassing FB.
3. To capture or stop and spoil the momentum and energy of any large particulates in the exhaust stream.
4. To absorb some of the energy from the exhaust jet by phase change of its materials.
5. To radiate some of the energy of the attenuated and diffused jet to the next outer barrier, the filter bag (FB).

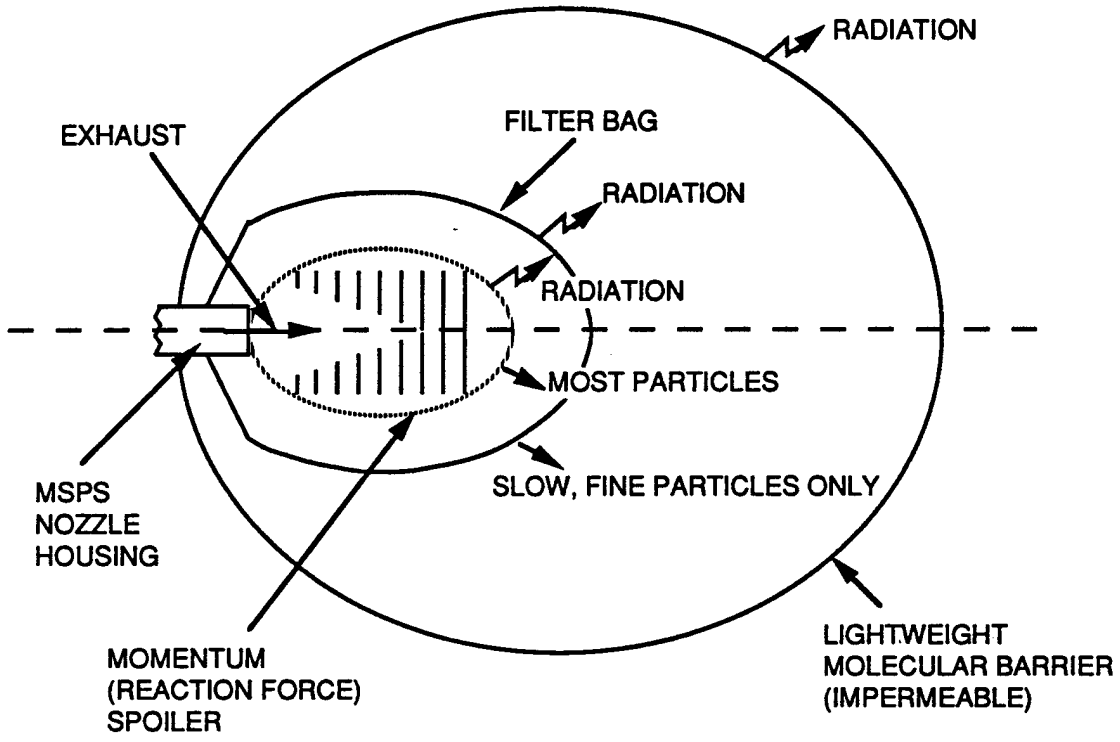

Fig. 1. Schematic of typical TECS configuration for use with the STD Research Corporation MHD Space Power System (STD/MSPS). Energy of exhaust is radiated to space from outer bladder which consists of a lightweight molecular barrier and a force containment structure (the latter not shown). Reaction forces are cancelled by the momentum spoiler. Coarse particulates are captured by filter bag. Fine, slow-moving particulates are cooled on the way to molecular barrier and are captured by it. Radiation flux from the molecular barrier to the surroundings cools the contained gas and the molecular barrier.

9-9050

The gases issuing from the MS are still quite energetic but diffuse. As the temperature of the stream is reduced by expansion, a large number of particulates condense, mostly in the 1–3 μm range, as was shown by Hoglund (Ref. 1). The now diffuse exhaust, with most of its energy and momentum spoiled and distributed evenly over a large area, encounters the FB — also made from specially treated lightweight commercially available high temperature materials — which serves three functions:

1. It further slows down and diffuses the momentum of gases and particulates that emerge from the MS and transmits their force to the MSPS.
2. It filters out all but the very finest of the now slowed-down particulates from the exhaust gases.
3. It radiates the greatest part of the energy of the exhaust to the next outer and final barrier, the molecular barrier (MB).

The surface of the filter bag is typically of the order of 100 to 1,000 times larger than the cross-sectional area of the exhaust.

The now very diffuse and slow-moving exhaust gases and the finest particulates from the exhaust encounter the nearly spherical MB, which stops them completely. The functions of the MB are:

1. To stop and contain all gases and the finest particulates from the exhaust of the MSPS.
2. To transmit and cancel any remaining reaction forces to the MSPS structure.
3. To radiate to space all the energy in the MSPS (or other power generator) exhaust — other than the energy absorbed by the MS and FB materials.

The MB is made of specially treated commercial materials that consist of an inner thin-wall bladder of impermeable metal foil and an outer force containment structure consisting of lightweight, high-temperature, high-strength filament-wound or woven fiber. Its surface area depends on many parameters, but it is of the order of 3,000 to 10,000 times the MSPS exhaust cross-sectional area.

All these components, including the woven-fiber/metal-foil force containment structure, have been successfully tested in small-scale model simulators under conditions that exceed those required by the STD/MSPS, albeit in separate experiments (*i.e.*, not in one integrated structure). For example, in order to avoid building the expensive facility and force containment structure required to test the complete integrated system, the conceptual design of the integrated molecular barrier, filter bag, and reaction force/energy spoiler were tested without the force-containment structure by venting the molecular barrier as shown in Fig. 5 and ensuring that less than 10% of the energy in the simulated MSPS exhaust escaped through the vent and the arcjet housing structure.

3. PROJECT DESCRIPTION

The objectives of this study were: (a) to carry out analytical investigations and computer simulations of a space-deployment-capable, complete effluent-and-reaction-force containment concept, the TECS concept, including its scaling laws and its response to dynamic stress and heat loads, (b) to investigate candidate materials for construction of the momentum spoiler (MS) and filter bag (FB) components of this MSPS subsystem in the STD Research high-enthalpy plasma flow facility, (c) to construct and test a model TEC system in the STD Research high-enthalpy plasma flow facility in order to resolve any identified technical uncertainties, (d) to prepare a conceptual design of a TEC system for any size MSPS to a level of detail that permits the gross system mass and costs to be determined within ± 20%, (e) to determine the suitability of this TEC system for space deployment and (f) to identify any remaining technical uncertainties and make recommendations for their resolution in larger-scale ground tests. The TEC system is designed for minimum size and weight.

To achieve these objectives, STD Research Corporation carried out the following three tasks:

- Task 1. Conceptual Design
- Task 2. Experimental Investigation
- Task 3. Reporting

The first two tasks are described, along with the results of this research program, in the following chapters of this Final Technical Report.

CHAPTER II

TASK 1: CONCEPTUAL DESIGN

1. SUBTASK 1.1: ANALYTICAL INVESTIGATIONS

The objectives of this subtask were to carry out analytical investigations and computer simulations of a preliminary conceptual design of a Total Exhaust Containment (TEC) system capable of deployment in space to contain all primary exhaust (aluminized fuel plus oxidant) effluents and cancel all reaction forces generated by the MHD Space Power System (MSPS) proposed by STD Research Corporation in response to DOE RFP DE-RP22-86PC90270.

The following sections address these objectives.

1.1 TECS Thermodynamic and Heat Transfer Models

1.1.1 *Perfect Gas Steady-State Model of the TECS Concept*

Studies of simplified thermal models of the steady-state and time-dependent behavior of the TEC system have been previously disclosed (*e.g.*, in STD-SP-001-87 of 27 January 1987, responding to PRDA RA22-87PC90271). This section presents the principal assumptions, equations, and numerical results from these studies in summary form.

These preliminary simplified TECS models were based on the energy balance (MHD effluent gas thermal input and radiated output) for a thin impermeable spherical bag (the molecular barrier) constructed of a uniform wall material that has negligible heat capacity and negligible thermal resistance. The MHD effluent is treated as an ideal gas; solid and liquid components of the effluent are ignored, *i.e.*, are assumed not to contribute significantly to the volume of the effluent gases contained in the impermeable bag, provided the temperature and pressure of the bulk of the gases in the bag allows them to exist as solids or liquids. However, their contribution the incoming enthalpy *is* accounted. The bag material is assumed to be a gray body with emissivity ϵ that radiates to empty space. It is also assumed that no radiation is incident on the bag from outer space and that the bag is in thermal equilibrium with the gas inside at all times. The validity of these assumptions is discussed at the end of Section 1.1.2.

The equation of state $pV = n\mathcal{R}T$ gives one relationship between the bag volume V and the time varying temperature $T(t)$, pressure $p(t)$ and number of moles $n(t)$ of the gas in the bag. If the bag is assumed to be spherical, its volume V and surface area A_S are directly related to its radius r; $\mathcal{R}$ is the universal gas constant. The MHD effluent flow begins at time $t = 0$ and ends when the flow is shut off at $t = t_f$.

The rate of radiative energy transfer from the spherical bag to its surroundings is given by

$$\dot{Q}_R(t) = 4\pi r^2 \sigma_B \epsilon (T(t))^4 \quad , \tag{1}$$

where σ_B is the Stefan-Boltzmann constant. Assuming steady-state conditions during operation, *i.e.*, that the effluent properties and flowrate are constant with time, and that the bag is initially empty, then the total energy $E(t_f)$ of the gas within the bag at burn completion is given by:

$$E(t_f)) = E_{th} - \dot{Q}_R t_f \quad , \tag{2}$$

where E_{th} is the total thermal output of the MHD effluents for $0 < t < t_f$. The thermodynamic relationship

$$p(t)V = (\gamma - 1)E(t) \quad , \tag{3}$$

with γ the ratio of specific heats of the cooled effluent gas in the bag, yields another equation relating the thermodynamic variables with the volume of the bag.

For the purposes of this calculation, it is assumed that the bag wall thickness t_w is the minimum value that will prevent the bag from bursting. Therefore, the thickness t_w can be obtained from the thin shell stress formula for spherical geometry and is given by:

$$t_w = \frac{p(t_f)r}{2S_w} \quad , \tag{4}$$

where S_w is the tensile strength of the bag wall material. Usually, if the material is wound or woven, its tensile strength is one-half or less of the net fiber tensile strength. The total mass M of the bag is

$$M = 4\pi r^2 t_w \rho_w \quad , \tag{5}$$

where ρ_w is the density of the wall material. Replacing t_w from the value given by Eq. (4), the mass of the bag can be expressed as:

$$M = 4\pi r^2 \rho_w \left(\frac{p(t_f)r}{2S_w}\right) = \left(\frac{3\rho_w}{2S_w}\right) p(t_f)V = \frac{3\rho_w n(t_f)\mathcal{R}}{2S_w} T \quad , \tag{6}$$

where the equation of state has been used to obtain the last equality. Thus, the total mass of the bag can be expressed either in terms of the final pressure and the bag's constant radius *or* the final pressure and the bag's constant volume *or* the final temperature *only*.

For STD Research Corporation's proposed 100 MW_e/500 s MHD Space Power System device, $n(t_f) = 4.68 \times 10^5$ mol = 468.3 kg–moles. Then, assuming bag material properties as $\rho_w = 1730\ \mathrm{kg/m^3}$ and $S_w = 396$ ksi, Eq. (6) becomes

$$M = (3.70\ \mathrm{kg/K}) \times T \qquad \text{(STD/MSPS)}. \tag{7}$$

Note that this relationship depends only on the steady-state or final temperature T of the gas within the bag, which, as will be shown in the next section, is reached very quickly. The following table shows some numerical examples computed using this simplified model with the bag material properties and effluent flow conditions taken as listed above, and

with a choice of $T = 1{,}000$ K and $M = 3{,}700$ kg. The computation is performed for several values of E_{th}, ϵ, and γ. Also tabulated are the maximum gas pressure $p(t_f)$ at burn completion, and required bag wall thickness t_w to hold this pressure. The results show that, in the first approximation, the required bag radius is nearly independent of the gas specific heat ratio, but depends very much on the emissivity of the radiating surface of the bag. It should also be noted that the estimate of bag mass obtained from this analysis is conservative since it is assumed that the energy carried in the bag by all the effluents is converted into *gas* internal energy *only*.

$E_{th} = 6\times10^{10}$ J		
ϵ	$\gamma = 1.2$	$\gamma = 1.4$
1.0	$r = 10.67$ m $p_f = 7.56$ atm $t_w = 1.50$ mm	$r = 11.88$ m $p_f = 5.47$ atm $t_w = 1.21$ mm
0.5	$r = 15.09$ m $p_f = 2.67$ atm $t_w = 0.75$ mm	$r = 16.8$ m $p_f = 1.94$ atm $t_w = 0.60$ mm

$E_{th} = 2\times10^{11}$ J		
ϵ	$\gamma = 1.2$	$\gamma = 1.4$
1.0	$r = 22.51$ m $p_f = 0.80$ atm $t_w = 0.34$ mm	$r = 23.11$ m $p_f = 0.74$ atm $t_w = 0.32$ mm
0.5	$r = 31.84$ m $p_f = 0.28$ atm $t_w = 0.17$ mm	$r = 32.68$ m $p_f = 0.26$ atm $t_w = 0.16$ mm

1.1.2 *Perfect Gas Time-Dependent Model of the TECS Concept*

For a more accurate estimate of the feasibility and capabilities of the TECS concept, it is necessary to solve the time-dependent mass and energy balance equations over the appropriate range of parameters. This will yield, for example, the final temperature required to estimate the mass of the bag.

For this model, the properties of the gas within the bag are assumed to be spatially uniform. The subscripts i and f refer to conditions at the start ($t = 0$) and the end of the burn ($t = t_f$), respectively.

The effluents entering the bag have a stagnation enthalpy H_0 and a stagnation temperature T_0. It is assumed that the condensible (liquid and solid) effluents make a negligible contribution to the volume and pressure in the bag. Therefore, only the gas component of the effluents contributes to the pressure within the bag. The internal energy of the gas within the bag can be obtained from the perfect gas law as:

$$E = \frac{RT}{\gamma - 1} \quad , \tag{8}$$

where R is the gas constant and γ the ratio of specific heats of the cold effluent gas in the bag. The gas constant R can be obtained from the universal gas constant $\mathcal{R}$ using $R = \mathcal{R}/\mathcal{M}$, where $\mathcal{M}$ is the molecular mass of the gaseous component of the contained effluents. All the energy in the exhaust is assumed to be carried by the gas only.

Now, consider the filling of a constant volume spherical vessel of radius r with thin impermeable walls by the gaseous exhaust of an open-cycle power generator. The mass balance for the gas in the bag can be written as:

$$\frac{d}{dt}(\rho V) = \dot{m}_{gas} \quad , \tag{9}$$

where ρ is the density of the gas within the bag and $\dot{m}_{gas}$ is the incoming mass flow rate of gas ($\dot{m}_{tot}$ is the total mass flow rate of effluents), assumed constant throughout the operating period (burn time or power pulse) of the generator. This last assumption is likely to hold since the pressure in the bag never rises to the point where the flow stops being supersonic at the exit of the generator.

Clearly, Eq. (9) integrates from $\rho = \rho_i$ at $t = 0$ to

$$\rho = \rho_i + \frac{\dot{m}_{gas}}{V} t \tag{10}$$

after a time t. The energy balance for the fluid within the bag is given by

$$\frac{d}{dt}(\rho V E) = \dot{m}_{tot} H_0 - \dot{Q}_R \ . \tag{11}$$

This formulation neglects the heat capacity of the bag wall material.

Eq. (11) transforms into

$$\rho \frac{dE}{dt} + E \frac{d\rho}{dt} = \frac{1}{V} \left(\dot{m}_{tot} H_0 - \dot{Q}_R \right) \tag{12}$$

and since $d\rho/dt = \dot{m}_{gas}/V$, then

$$\rho \frac{dE}{dt} = \frac{\dot{m}_{gas}}{V} \left(\frac{\dot{m}_{tot}}{\dot{m}_{gas}} H_0 - E - \frac{\dot{Q}_R}{\dot{m}_{gas}} \right) \ . \tag{13}$$

Defining ϖ as the ratio of gas mass flow rate to total effluent mass flow rate, *i.e.*,

$$\varpi = \frac{\dot{m}_{gas}}{\dot{m}_{tot}} \tag{14}$$

and assuming that the ideal and perfect gas laws apply, we can obtain

$$\rho \frac{dT}{dt} = \frac{\dot{m}_{gas}}{V} \left[\left(\frac{\gamma - 1}{\varpi R} \right) H_0 - T - \left(\frac{\gamma - 1}{R} \right) \frac{\dot{Q}_R}{\dot{m}_{gas}} \right] \ . \tag{15}$$

Then, by use of Eq. (10) and Eq. (1) we obtain

$$\frac{V}{\dot{m}_{gas}} \left(\rho_i + \frac{\dot{m}_{gas}}{V} t \right) \frac{dT}{dt} = \left[\left(\frac{\gamma - 1}{\varpi R} \right) H_0 - T - \frac{(\gamma - 1) \epsilon \sigma_B T^4 A_S}{R \dot{m}_{gas}} \right] \ . \tag{16}$$

Now, if we define the characteristic time $\tau_0 = \rho_0 V / \dot{m}_{gas}$, where ρ_0 is the stagnation density, we obtain

$$\tau_0 \left(\frac{\rho_i}{\rho_0} + \frac{t}{\tau_0} \right) \frac{dT}{dt} = \left(\frac{\gamma - 1}{\varpi R} \right) H_0 - T - \frac{(\gamma - 1) \epsilon \sigma_B T^4 A_s}{R \dot{m}_{gas}} \ . \tag{17}$$

After the transformations

$$x = t/\tau_0 \, , \tag{18}$$

and

$$y = T/T_0\,, \tag{19}$$

we obtain

$$\frac{dy}{\left(\frac{\gamma-1}{\varpi R}\right)\frac{H_0}{T_0} - y - N_R y^4} = \frac{dx}{(\rho_i/\rho_0) + x}\,, \tag{20}$$

where the dimensionless parameter N_R is given by

$$N_R = \frac{(\gamma-1)\epsilon\sigma_B T_0^3 A_S}{R\dot{m}_{gas}}\,. \tag{21}$$

The integration of Eq. (20) yields values for the pressure and temperature of the gas in the bag as a function of time. A computation has been performed for the following values of the appropriate parameters, which are relevant to the STD/MSPS:

$\mathcal{M} =$	31.83 kg/kg-mole	$\dot{m}_{gas} =$	29.81 kg/s*
$H_0 =$	8 MJ/kg	$\varpi =$	0.60
$\rho_0 =$	0.10 kg/m^3	$\rho_i \approx$	0 kg/m^3
$\epsilon =$	0.1, 0.5, and 1.0	$\gamma =$	1.1, 1.2, 1.3, and 1.4

The following tabulation gives the final temperature for two TEC systems of radius $r = 23.5$ m and 35 m, respectively, as a function of γ and ϵ:

		$\gamma = 1.1$	$\gamma = 1.2$	$\gamma = 1.3$	$\gamma = 1.4$
$r = 23.5$ m	$\epsilon = 0.1$	1623	1706	1733	1746
"	$\epsilon = 0.5$	1122	1158	1170	1176
"	$\epsilon = 1.0$	954	979	987	991
$r = 35.0$ m	$\epsilon = 0.1$	1355	1410	1428	1437
"	$\epsilon = 0.5$	931	955	963	967
"	$\epsilon = 1.0$	789	806	812	816

This time-dependent model showed that the bag temperature approaches the steady-state value derived from the steady-state energy balance in a few (typically less than 10) seconds, and it has been used to simulate in time the thermal behavior of the system for a range of initial conditions. Cases were examined in which the bag contains an initial amount of gas of density ρ_i that is very small compared to the final density. The effect of a finite initial gas density (as well as finite thermal mass of other TECS components, as shown later) was found to cause the bag temperature to rise more slowly from its initial value as it approaches an asymptotic final value $T = T(t_f)$. This asymptotic value is equal to the value predicted by the steady-state model. These time-dependent studies indicated that brief fluctuations in effluent flow conditions at generator start-up are not expected to produce destructive transient temperatures greater than the asymptotic, *i.e.*, design temperature of the TECS bag.

* This is the mass flow rate of gas for a total mass flow rate of 50 kg/sec for a typical aluminized fuel.

In reality, the molecular barrier will contain small-size particles along with the MSPS effluent gases. Since the transfer of energy from the filter bag to the molecular barrier is mainly by radiation, the radiation-absorbing gas-particle mixture is likely to be at a higher temperature than that of the molecular barrier. As is shown in Section 1.1.3.2 for the analysis of the radiative energy transfer between the filter bag, the molecular barrier and the gas-particle cloud in between, the temperature of the effluents within the bag is nearly independent of their emissivity and is at most 20% higher than that of the bag for typical cases. Since the pressure rise inside the bag is proportional to the effluent temperature, an effluent temperature 20% higher than what is assumed in the simple analysis presented above implies a TECS mass 20% higher than predicted by Eq. (7). However, it is assumed in the above that all the energy (stagnation enthalpy) of the exhaust is contained in the exhaust gases. This is a conservative assumption because the particulate matter, which makes a negligible contribution to the pressure-volume relationship, will be approximately 40% of the total effluent mass and at about the same temperature as the contained gases and therefore may contain a comparable amount of energy as the gas.

1.1.3 *More Elaborate TECS Models*

In this section, more elaborate TECS thermodynamics and heat transfer models are presented. In order to refine the weight estimate obtained in the previous section, it is necessary to include effects of finite thermal conductivity and heat capacity of the molecular barrier/force containment structure assembly, and to examine the radiative heat transfer between the FB and the MB in presence of an absorbing medium (*i.e.*, the contained effluents) in between. The effects of the inlet duct components (diffuser/heat exchanger and MS) are ignored except as they affect the total thermal input to the system and radiative transfer efficiency of the various surfaces.

1.1.3.1 *Effects of Finite Thermal Conductivity and Heat Capacity of Bag Wall.*

In order to be applicable to as wide a range of materials properties and mission parameters as possible, this TECS model does not assume that the temperature drop across the containment bag wall is small. The more elaborate TEC system model presented here for calculating the system energy balance extends and refines the preliminary steady-state and time dependent models in the following ways: the single bag is replaced by a more realistic structure comprising a thin impermeable foil backed up by a composite force containment structure. It is assumed that this assembly has a finite heat capacity c_w and a finite thermal conductivity k_w. The inner molecular barrier has a surface mass density η_c. There is also a smaller inner permeable filter bag (FB) that captures the solid or liquid particulate components of the MHD effluent to prevent abrasion of the containment bag wall. The containment bag outer surface (called surface 1) is assumed to be exposed to an average incident radiant flux $\dot{q}_1$ from outer space, and it is designed to support a pressure $f^* p_{max}$ without bursting, where f^* is a safety factor greater than one and p_{max} is the yield pressure of the bag. Other assumptions of the preliminary time-dependent model, such as thermal equilibrium and ideal gas equation of state, are retained in this model.

Fig. 2 shows diagrammatically the convention followed in this study for numbering the bag wall surfaces in this and the following models. As before, the subscript 0 refers to

the stagnation properties of the incoming MSPS effluents. The outer and inner surfaces of the containment bag are respectively labeled as surfaces 1 and 2, while the outer and inner surfaces of the permeable filter bag are labeled surfaces 3 and 4, respectively.

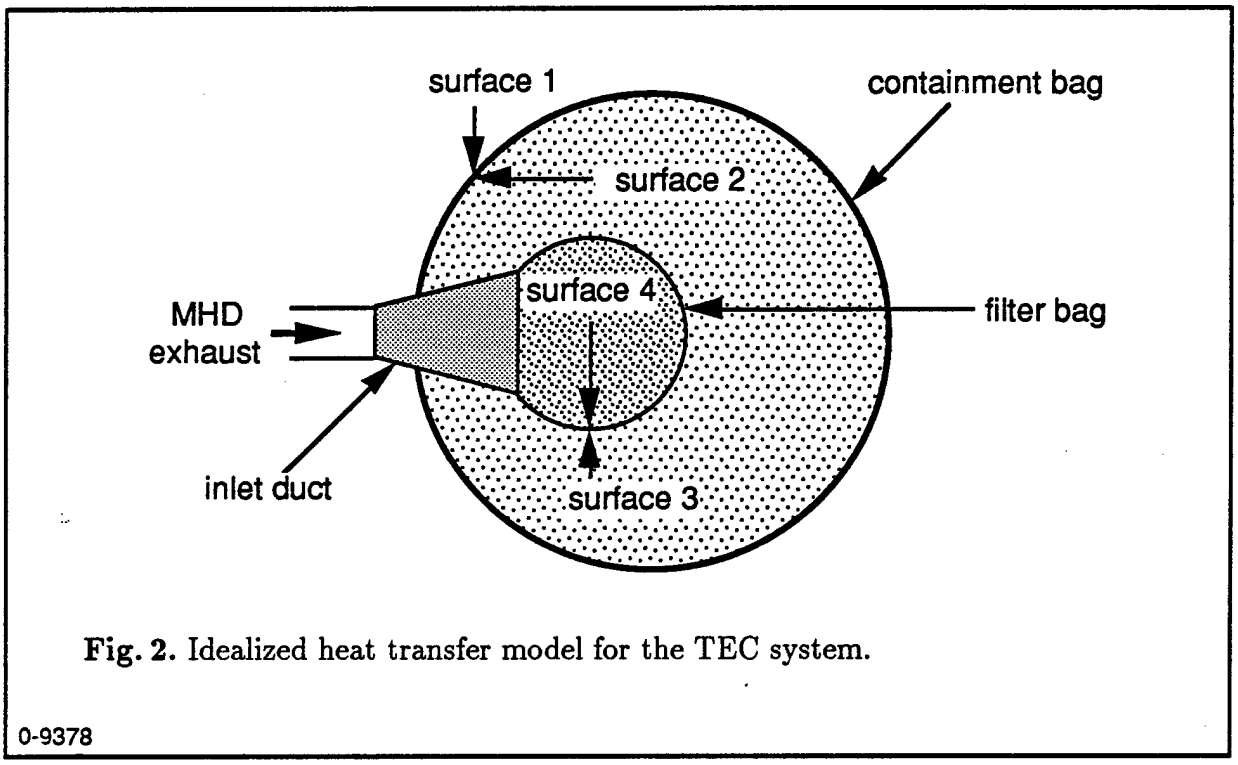

Fig. 2. Idealized heat transfer model for the TEC system.

The containment bag wall material characteristics used for modeling purposes are based on the assumption that the outer wall is at a uniform temperature $T_1(t)$ and that the inner wall is at a uniform temperature $T_2(t)$. The properties and thickness of the containment bag material are assumed to be constant over its surface. If woven fabric is used as the principal structural component of the bag wall, then the fabric characteristics ρ_w, S_w, and k_w may have values somewhat lower than the corresponding values for density, tensile strength, and thermal conductivity of the fibers from which the fabric is woven.

For *steady effluent flow conditions* for $0 < t < t_f$ with $n(0) = 0$ and $c_w = 0$, the following equations describe this model for $0 < t < t_f$:

$$\dot{Q}_R = 4\pi r^2 \left(\sigma_B \epsilon_1 T_1^4 - \dot{q}_1\right) \quad \text{(gray-body radiation)} \tag{22a}$$

$$T_2 - T_1 = \frac{t_w/k_w}{4\pi r^2}\dot{Q}_R \quad \text{(wall heat conduction)} \tag{22b}$$

$$\dot{E}_{th} = \frac{\dot{n}\mathcal{R}T_0}{\gamma - 1} \quad \text{(ideal gas)} \tag{22c}$$

$$\frac{\dot{n}\mathcal{R}T_2}{\gamma - 1} = \dot{E}_{th} - \dot{Q}_R \quad \text{(energy balance).} \tag{22d}$$

(In Eqs. (22), the explicit time-dependence of quantities is not shown; all quantities displayed are constant for $0 < t < t_f$ for the steady-state case). Eliminating $\dot{Q}$ and $\dot{E}_{th}$ from Eqs. (22) yields

$$\frac{\dot{n}\mathcal{R}}{(\gamma-1)}(T_0 - T_2) = 4\pi r^2 \left(\sigma_B \epsilon_1 T_1^4 - \dot{q}_1\right) \quad , \tag{23a}$$

$$T_2 - T_1 = \frac{\dot{n}\mathcal{R}t_w/k_w}{4\pi r^2(\gamma-1)}(T_0 - T_2) \quad . \tag{23b}$$

The equation of state $p(t)V = n(t)\mathcal{R}T(t)$ gives the gas pressure $p(t)$ in terms of the gas temperature $T(t)$. For steady effluent flow $n(t) = \dot{n}t$ and $T_2(t) = T_2$, and therefore the equation of state implies that the gas pressure at generator shutdown, defined by $p_f = p(t_f)$, is the highest gas pressure reached for $0 < t < t_f$. For a spherical bag $V = 4\pi r^3/3$, so the equation of state becomes

$$p_f = \frac{3\mathcal{R}}{4\pi r^3}\dot{n}t_f T_2 \quad . \tag{24}$$

The pressure-limited wall thickness t_w^* is the wall thickness that would cause a spherical bag, made of material with tensile strength S_w, to burst at the pressure $f^* p_f$. The pressure-limited wall thickness is thus determined by the formula $\pi r^2 f^* p_f = 2\pi r S_w t_w^*$, which, combined with Eq. (24), yields

$$t_w^* = \frac{3\mathcal{R}}{8\pi r^2}\frac{f^*}{S_w}\dot{n}\, t_f\, T_2 \,. \tag{25}$$

Finally, the total bag mass M is the sum of the masses of the containment bag structural wall layer and the impermeable molecular barrier layer:

where

$$M = 4\pi r^2(t_w \rho_w + \eta_c), \tag{26a}$$

$$t_w = \max(t_w^*, t_{w,\min}). \tag{26b}$$

From other design considerations, the minimum allowable wall thickness is $t_{w,\min}$. Note that the masses of the filter bag and other minor structures are not included in M.

In summary, since the composite bag wall thickness is very small, the inner and outer surfaces approach the same temperature very rapidly. The final temperature of the gas in the sphere will also be reduced since energy is absorbed by the bag material if its heat capacity is non-zero. However, this effect is likely to be very small.

1.1.3.2 *Effects of Contained Effluents on Radiative Energy Transfer.*

We have also performed a steady-state analysis of the radiative heat transfer between the filter bag and the molecular barrier in the presence of an absorbing medium, *i.e.*, a particle-gas mixture. This is a heat flux conservation analysis which neglects the heat capacity of the contained effluents (*cf.* Refs. 2 and 3). The main arguments and results are summarized here.

For this analysis the FB, the MB and the contained effluents are modeled as grey bodies. The transmittivity of the FB and MB along with the reflectivity of the gas-particle mixture are assumed to be zero. The problem is analyzed with the help of an electrical analog where the potentials are replaced by radiosities, the currents by heat transfer rates and the radiative resistance of each component is a function of its geometry and emissivity. The electrical analog for the problem at hand is shown in Fig. 3. It is found that, since there is a relatively large surface area ratio between the MB and FB, the temperature of the contained effluents is nearly *independent* of their emissivity. However, the effluent temperature is sensitive to the emissivity of the MB. A computation performed for the TECS relevant to the STD MSPS revealed that the temperature of the contained effluents is always about 200K above that of the MB. Applying this to the steady state analysis of Section 1.1.1, this means that the mass of the TECS bag should be 20% higher than predicted by Eq. (7), *i.e.*,

$$M = (4.44\,\mathrm{kg/K}) \times T_{bag} \qquad \text{(STD/MSPS)}. \tag{27}$$

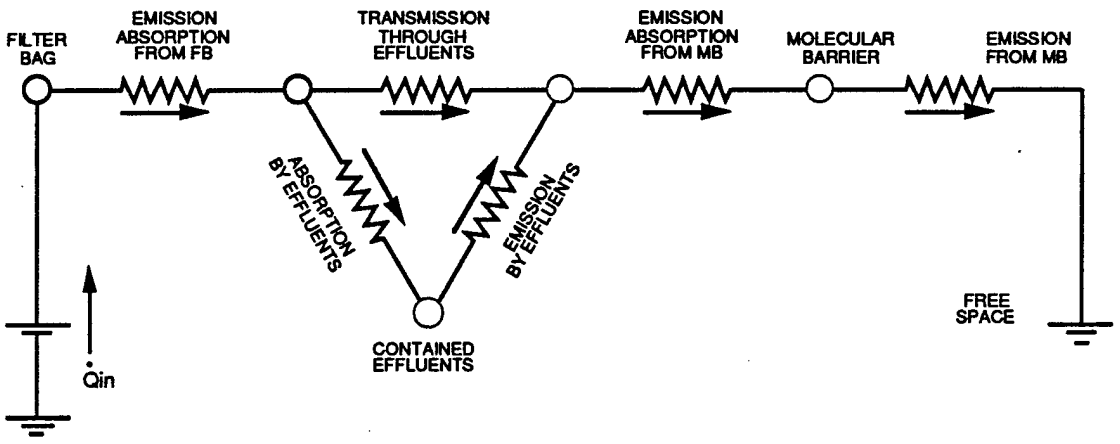

Fig. 3. TECS model for radiative heat transfer between the FB, the MB and the contained particles/gas in between.

However, both the present analysis and that of Section 1.1.1 assume that all the MSPS effluent energy has to be radiated into free space. In reality, a portion of it, almost 10%, is absorbed by sublimation of the MS as it is eroding, and by heating up all of the TECS components and the contained effluents. Furthermore, even though the velocity of the effluents is reduced as they pass through the MS and FB, there will be some convective heat transfer between the gas/particle cloud and the MB. In light of these effects, the mass estimate given by Eq. (27) is considered to be conservative.

1.1.3.3 *Effects of Surface Spectral Emissivities.*

A model for computing the radiant transfer between the filter bag and containment bag had also been developed to investigate the process of selection of a bag wall molecular barrier. The basic assumptions and conclusions of this analysis are presented here.

For the purposes of this examination, it is assumed that: (a) surface 3 (*i.e.*, the outer surface of the filter bag) has a fairly high emissivity and can be considered a gray body, (b) $T_3 > T_2$, (c) surface 2 (*i.e.*, the inner surface of the molecular barrier) is a metallic layer whose radiative properties can be modified, *e.g.*, by oxidation or anodization, on the interior side or on both sides to increase absorptivity, and (d) that the contained effluents are transparent to all radiated wavelengths. Surface 2 is *not* assumed to be a gray surface. For example, the normal emissivity of anodized aluminum varies by a factor of nearly 3 or more in the narrow wavelength range $2\ \mu m < \lambda < 5\ \mu m$, so it is very far from being accurately modeled as a gray surface.

Results show that heat transfer is enhanced if the specific emissivity of surface 2 (inside) is a decreasing function of wavelength λ, compared to a gray body of equal average emissivity. This occurs because surface 3, being hotter than surface 2, emits radiation at relatively short wavelengths. A smooth decrease of the specific emissivity of surface 2 with λ is characteristic of electrical conductors (pure, unoxidized metals). Therefore, it is desirable for surface 2 to have low specific emissivity for the wavelengths at which it is emitting to decrease its tendency to return radiant energy to the bag interior, provided: (a) the absorptivity of surface 2 at wavelengths emitted by surface 3 is high and (b) the outward heat transfer from the molecular barrier to the structural bag wall is mainly by conduction or by radiation with a higher emissivity than that of surface 2. Thus, good thermal contact between the inner barrier and the outer structural (*e.g.*, graphite composite) layer of the bag wall is necessary to take full advantage of a metallic molecular barrier material.

It is expected that the specific emissivity of the outer side of a metallic molecular barrier would be smaller than the emissivity of graphite at wavelengths of interest, so it may make more sense to treat the *outer* side, rather than the inner side, of the molecular barrier (at the interface with the structural material) to increase its thermal contact and emissivity at temperature T_2. It is also expected that the gas pressure will produce excellent mechanical and thermal contact between the molecular barrier and structural wall materials. Therefore, it is found that the force containment structure for the molecular barrier should be placed on the outside (low pressure side) rather than on the inside. These issues need to be quantified experimentally.

1.1.3.4 *Influence of These More Elaborate Models on TECS Mass and Performance.*

Briefly, the principal qualitative effects of the more detailed and realistic features included in the more elaborate TECS models, as described in the previous sections, can be summarized as follows:

1. The non-negligible containment bag wall heat capacity c_w increases the thermal rise time, *i.e.*, the time required to heat up the structure of the system, yielding a reduction in the start-up thermal stresses. A typical rise time estimated for the

STD/MSPS TECS is a few (5–10) seconds. There are no significant structural stresses on the containment bag in this time interval.

2. A finite containment bag wall thermal conductivity k_w places an upper limit on the containment bag outer surface temperature T_1. This effect is greater for small, hot designs (low r, high T) due to the high through-the-wall heat flux and correspondingly large temperature drop in the containment bag wall. For the STD/MSPS TECS, this temperature drop is estimated to be 1 K or less, a negligible value. But this effect could be very important for different mission parameters.
3. The molecular barrier surface mass density η_c limits the maximum size of the TECS bag. In the preliminary model, the mass of the structural wall decreases with r, since a larger bag has a lower final pressure and therefore a thinner wall. Therefore, the preliminary model system mass M was limited only by the minimum wall thickness $t_{w,\min}$. In the more elaborate model, M includes the mass of the molecular barrier membrane (thin metal film), which increases with r. In the STD/MSPS TECS, the mass of the thin metal film is small compared to the mass of the force containment structure. Progress in manufacturing thinner structural walls must go hand-in-hand with progress in applying thinner molecular barriers to produce further reductions in total system mass.
4. The decrease of specific emissivity with wavelength, characteristic of most electrical conductors, makes metallic film more attractive as a molecular barrier than one might expect from simple gray-body computations based on average emissivity data.
5. Absorption/emission by the contained effluents causes them to be at a higher temperature than the molecular barrier. The temperature difference between the MB and the trapped gases and particles is nearly independent of the gray body emissivity of the latter two, and is at most 20% of the MB absolute temperature.

1.1.4 *Summary*

These results suggest a number of promising approaches to further reduce the TECS system mass through continued careful analyses and materials selection, such as tailoring the spectral emissivity of the molecular barrier/ force containment structure assembly. Further computational and experimental effort is also required to verify and extend this work, for example by performing a full spectral and time-dependent computation of the radiative heat transfer within the TECS, including convective and conductive effects, energy retained by the solids and particulates and published material properties.

From the analyses of the TECS concept performed above, the mass of the bag is best computed using Eq. (27). It is a conservative estimate.

2. SUBTASK 1.2: SCALING ANALYSES

The objectives of this subtask were to analyze and present the appropriate scaling laws for scaling the size of this device with power level, firing time and total energy.

2.1 Scaling Laws

From very simple physical arguments concerning the physical processes governing the operation of the TECS concept, scaling laws can be derived to determine the dimensions and weight of any size system, once a conceptual design for a TEC system of a certain size has been established.

2.1.1 *Assumptions*

In the derivation of the scaling laws for TECS systems, it is assumed that:

1. The properties of the effluents exhausting from the diffuser of the MHD generator are the same for any size device.
2. The time taken to achieve steady-state operation is small compared to the overall operating time t_f. As seen in Section 1.1.2, this is a good assumption and therefore the steady-state analysis presented in Section 1.1 will be used.
3. All TECS systems are fabricated from the same materials.
4. The steady-state temperature of the gases inside the molecular barrier is the same for all cases.
5. The steady-state pressure of the gases inside the molecular barrier is such that the stresses in the material forming the molecular barrier are the same for all cases.
6. Scaling of all radiative parameters is accounted for by the derating factor applied to Eq. (7), to obtain Eq. (27), which approaches one as the scale of the device gets smaller (see Section 3 at the end of this Chapter).

These simple assumptions should hold for most instances.

2.1.2 *Results*

The scaling laws presented in this section are based on the steady-state analysis of the previous chapter, with the use of the assumptions listed above.

From simple geometrical considerations, it is first found that if the area of the momentum spoiler A_{MS} is to be proportional to the exit area of the MHD diffuser A_e, the distance ℓ initially separating the momentum spoiler from the exit of the diffuser has to scale with the square root of the exit area. Therefore,

$$A_{MS} \propto A_e \tag{28}$$

and

$$\ell \propto A_e^{1/2} \tag{29}$$

From momentum spoiler erosion considerations, its thickness L_{MS} scales with the total operating time, *i.e.*,

$$L_{MS} \propto t_f \tag{30}$$

Therefore the mass of the momentum spoiler scales as:

$$M_{MS} \propto A_e t_f \tag{31}$$

From the proposed design for the momentum spoiler-filter bag arrangement, it is easily seen that the filter bag has to scale directly from the dimensions of the momentum spoiler. Thus, the mass of the filter bag M_{FB} scales as:

$$M_{FB} \propto A_e t_f \tag{32}$$

All dimensions of the support structure of the momentum spoiler-filter bag assembly also scale with the square root of the exit area. Furthermore, since the reaction force caused by the MHD exhaust jet is proportional to the exit area, the cross-section of the structural members also scales with the exit area. Therefore, the mass of the MS-FB support structure M_{SS} scales with the exit area as:

$$M_{SS} \propto A_e^{3/2} \tag{33}$$

From the steady-state analysis of Chapter II it can also be seen that, for the same exit conditions and bag temperature, the radius of the molecular barrier scales with the square root of the exit area, *i.e.*,

$$r \propto A_e^{1/2} \tag{34}$$

The thickness t_w of the molecular barrier scales as:

$$t_w \propto t_f \tag{35}$$

and therefore the mass of the molecular barrier scales as:

$$M_{MB} \propto A_e t_f \tag{36}$$

From Eqs. (31), (32) and (36) it is seen that, if the mass of the MS-FB support structure is neglected, which is a reasonable assumption, the mass M of a complete TECS system scales as:

$$M \propto A_e t_f \tag{37}$$

3. SUBTASK 1.3: DESIGN DEFINITION

The objectives of this subtask are to prepare a preliminary conceptual design of a TEC system for the size of MSPS of greatest interest to the government (*e.g.*, the system required in RFP No. DE-RP22-86PC90270) to a level of detail that permits the gross TEC system mass and costs to be determined to within ± 20% and determine the suitability of this TEC system for space deployment. Since the molecular barrier and its force containment structure contribute to most of the mass of the TECS, this section examines the optimization of the bag size.

Effects of the bag size on the final mass of the assembly has been examined using the purely radiative model developed in Section 1.1.3.2. Fig. 4 shows the bag and gas temperatures as a function of bag radius. Since a larger bag offers a larger surface area to radiate away the energy from the MSPS effluents, it can radiate at a lower temperature. The gas temperature, and its pressure, also decrease with increased radius. Therefore, the mass of the force containment structure decreases with bag size. In fact, it can be shown that the mass M_{FCS} of the force containment structure is inversely proportional to the square root of the bag radius, *i.e.*,

$$M_{FCS} \propto r^{-1/2} \quad . \tag{38}$$

Also plotted in Fig. 4 is the ratio of gas temperature to bag temperature, the so-called derating factor $\mathcal{K}$. This factor can be used to modify Eq. (7) to obtain a more realistic mass estimate as:

$$M = \mathcal{K}\,(3.7\,\mathrm{kg/K}) \times T_{bag} \qquad \text{(STD/MSPS)}. \tag{39}$$

This equation is similar to Eq. (27), where a derating factor of $\mathcal{K} = 1.20$ was used.

However, increasing the size of the bag to infinity does not decrease its mass to zero. Since the thickness of the foil making up the molecular barrier is fixed, its mass M_{MB} increases with the bag size as:

$$M_{MB} \propto r^2 \quad . \tag{40}$$

The mass of the bag assembly comprising the FCS and the MB can therefore be expressed as:

$$M_{bag} = \mathcal{A} r^{-1/2} + \mathcal{B} r^2 \quad , \tag{41}$$

where $\mathcal{A}$ and $\mathcal{B}$ are proportionality constant depending on MSPS and material parameters. The minimum bag mass is obtained by differentiating Eq. (41) with respect to r. The minimum bag mass is found to be:

$$M_{bag,min} = 4^{1/5} \left(1 + \frac{1}{4}\right) \mathcal{A}^{4/5} \mathcal{B}^{1/5} \quad , \tag{42}$$

at an optimum radius of

$$r_{opt} = \left(\frac{1}{4}\frac{\mathcal{A}}{\mathcal{B}}\right)^{2/5} \quad . \tag{43}$$

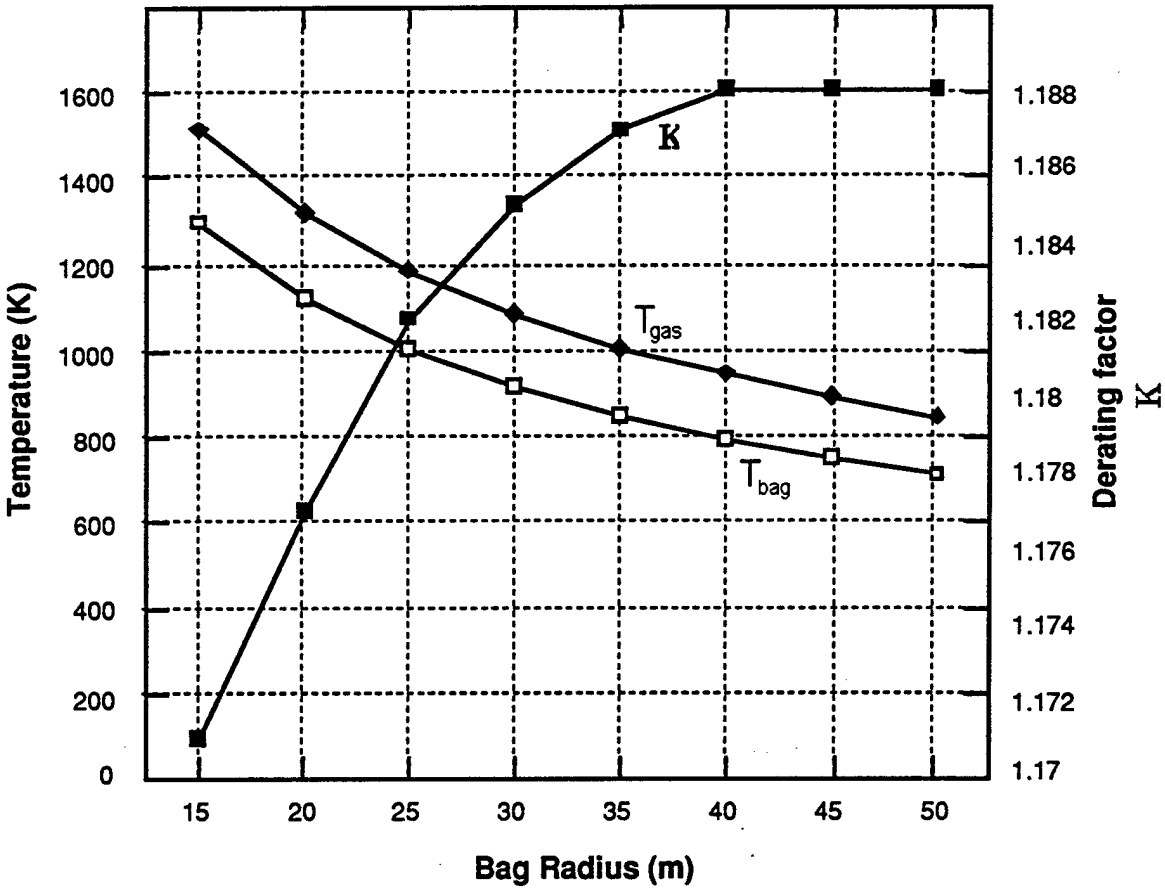

Fig. 4. Temperature of bag (T_{bag}) and contained gases (T_{gas}) as a function of bag radius; computation performed using the purely radiative model of Section 1.1.3.2, bag emissivity assumed as $\epsilon = 0.9$. Also plotted if the derating factor $\mathcal{K}$, defined as the ratio of gas temperature to bag temperature, *i.e.*, $\mathcal{K} \equiv T_{gas}/T_{bag}$.

0-9375

For a force containment structure having the properties listed in Section 1.1.1 and a molecular barrier foil having a thickness of 8×10^{-3} mm, the optimum bag size and mass can be found from Fig. 4 and the use of Eq. (39) and Eq. (42). If nickel is used as the foil material, then $r_{opt} = 33$ m and $M_{bag,min} = 4800$ kg. If aluminum is used as the foil material, then $r_{opt} = 53$ m and $M_{bag,min} = 3800$ kg.

The mass of the complete TEC system applicable to the STD/MSPS also includes the mass of the other components. The values listed in the previous paragraph should then be considered as rough estimates of the total mass of the TECS. However, these values can also be considered as conservative estimate for the mass of the bag assembly since, as stated in Section 1.1.3.2, effects of convective heat transfer and finite heat capacity

of the components and the particulates, as well as the heat of sublimation of the MS and FB reduce the final temperature and pressure of the contained gas. A more detailed conceptual design for the complete TECS is performed in Chapter III, Section 3 of the present report.

CHAPTER III

TASK 2: EXPERIMENTAL INVESTIGATION

This chapter describes the tasks that were performed and the results obtained in the experimental investigation of the TEC concept.

1. SUBTASK 2.1: MATERIALS SELECTION

The objectives of this subtask were to screen and select candidate materials for construction of the momentum spoiler (MS) and filter bag (FB) components of the TEC system and to evaluate their performance in the operating STD Research high-enthalpy (arcjet) plasma flow facility (HEPFF). This investigation included tests under vacuum (1–10 mmHg) conditions.

Testing of prospective materials for the MS and FB was conducted by subjecting a layer of material to the impingement of a 15 MJ/kg arcjet. The arcjet impinged the target material at 90° and the two were separated by a distance of 33 cm. The tests were performed for a 500-second duration and penetration of the target was observed visually. Materials tested included Transite, castable alumina, castable alumina-zirconia and carbon felt. The results of these experiments are shown in Table II. It is seen that the thinner materials all burned through before the end of the test and that most thicker materials lasted. STD Research Corporation also has experience with other high-temperature materials such as carbon phenolics and cork. However, carbon felt was judged to have outperformed all others since it had the lowest density. Therefore, carbon felt was chosen as the material for the construction of the MS and FB used in the subscale tests, and the same material is proposed for the full-scale device.

After material testing and screening, the emphasis was placed in arriving at an optimum configuration for the MS and FB components.

Three configurations were tried for the momentum spoiler. One was a cylinder placed with its axis perpendicular to the flow, but offset such that the arcjet impinged tangentially on one side. The idea was that the impinging jet would cause spinning of the cylinder to distribute the heat flux on the surface of the latter. When spinning around, the cylinder material would cool by radiation before reentering the impingement region. Experimental testing revealed that the cylinder kept accelerating under vacuum until it failed due to the large centrifugal forces. For this reason, this approach was abandoned.

A second configuration was tried for the MS. For this one, the MS was a hollow cone with the base closest to the arcjet. This was found to work, although this geometry

Table II. Screening of candidate materials for MS and FB components of the TECS. Testing performed under vacuum with 15 MJ/kg arcjet impinging on a layer of material at 90°, 33 cm away.

Material	Thickness (in)	Visual Observation after 500 s
Transite	0.125	burn through
	0.25	burn through
	0.5	burn through
	1.0	no burn through
Castable Al_2O_3	0.125	burn through
	0.25	burn through
	0.5	burn through
	1.0	no burn through
Castable Alumina-Zirconia	0.125	burn through
	0.25	burn through
	0.5	burn through
	1.0	no burn through
Carbon Felt	0.25	burn through
	0.5	burn through
	1.0	no burn through
	2.0	no burn through
	3.0	no burn through
	4.0	no burn through
	5.0	no burn through

was difficult to construct for the subscale experiments because the carbon felt material could not be bent properly in these small sizes. A similar conical configuration was tried, with the apex of the cone near the arcjet, with the same success and difficulties as the other conical configuration.

Finally, a final configuration for the MS was tried. For this one, the MS was cylindrical, with the base of the cylinder perpendicular to the axis of the arcjet. This was found to work and was selected for the subscale laboratory tests because it was easy to build.

The configuration of choice for the FB is a simple sphere, to provide a uniform radiation pattern. However, the manufacturing of a small sphere made out of carbon felt material for the subscale experiments proved to be too difficult. Therefore, in the subscale tests, the FB has a conical shape, as seen in Fig. 6.

2. SUBTASK 2.2: SUBSCALE MODEL TESTING

The objectives of this subtask were to design and construct a small-scale model of a TEC system and test it in the STD Research HEPFF under vacuum conditions.

TECS subscale simulators, designed by the simplest and crudest possible theory, namely the perfect gas steady-state theory of Section 1.1.1, have provided what is considered convincing proof of the technical feasibility of the TECS concept in the laboratory. During the course of this investigation it was found that the cost of building a subscale force containment structure for the molecular barrier was prohibitive and that the time required for it would have exceeded the duration of the contract. Therefore, a method was devised for testing the feasibility of all the components as sub-assemblies. The high-temperature performance of the MS, FB and MB was investigated in an integrated subscale simulator. This series of tests examined the feasibility of the MS alone, that of the MS with the FB and that of the MS, FB and MB together. In this latter series, the MB was vented to avoid pressure buildup, and therefore avoid the need for a force containment structure, in such a way that the energy carried away by the vented gases was small compared to the energy radiated by the MB. These tests simulated successfully the complicated interaction between the fluid mechanics of the hot exhaust plasma, the radiation field and the material properties of the components. The mechanical strength of the proposed force containment structure/molecular barrier assembly was successfully tested in a separate series of experiments. These tests were able to verify the technical feasibility of each component of a TEC system.

This proof was provided in a series of separate experiments using arcjets to simulate the MSPS exhaust in three separate flow facilities. These facilities consisted of:

1. A "clean" vacuum facility, where a pure nitrogen jet with enthalpies from a low of 8.21 MJ/kg to a high of 17.07 MJ/kg and a stagnation pressure of approximately 1.05 to 1.20 atm was fired against: (a) the momentum/energy spoiler (MS), (b) the MS plus the filter bag (FB), and (c) the MS plus the FB plus the (vented) thin-wall metal foil molecular barrier.
2. A "dirty" atmospheric facility, where aluminum oxide powder was mixed with the nitrogen jet to simulate the STD/MSPS exhaust at enthalpies of 14 to 15 MJ/kg of total effluents, including the Al_2O_3 and 4 to 5 atm gas-feed pressure (arcjet exhaust stagnation pressures not lower than 1.2 atmospheres). It was fired against the MS/FB assembly only, at atmospheric pressure.
3. A "dirty" vacuum to atmosphere facility, where aluminum oxide powder was mixed with the nitrogen plasma to simulate the STD/MSPS exhaust at enthalpies ranging from 13.3 to 13.8 MJ/kg of total effluents and 4 to 5 atm gas-feed pressure (arcjet exhaust stagnation pressure not lower than 1.2 atmospheres). It was fired against the MS/FB assembly only, at pressures around 0.8 atm.

During the performance of this contract, only the MS and FB components were tested in the "dirty" facilities. The atmospheric "dirty" facility was abandoned, for safety reasons, after several catastrophic failures of components other than and not related to

the TECS components, such as heat shields and inspection ports. Tests performed in this facility were just too dangerous for the observer.

A total of more than 15,000 seconds of test time of TECS devices and components at high enthalpy (about 13 MJ/kg or higher) has been accumulated. All the runs but two in the "clean" test tank exceeded 500 second test times at high enthalpy conditions.

All tests, on the average, were conducted under enthalpy conditions 50% higher, and in no case lower, than the MSPS exhaust enthalpy of 8 MJ/kg. In addition, the arcjet exhaust stagnation pressure was never lower than 130% of the expected MSPS exhaust stagnation pressure of 0.63 atm and the arcjet velocity was never lower than 200% of the MSPS effluents (650 m/s). In the early tests the indicated plasmajet enthalpy appeared to drop towards the end of these tests because of radiation from the TECS components to the arcjet housing and cooling systems, which artificially elevated the water exit temperature, and other reasons. This drop was analyzed and corrections were ultimately devised. Thereafter the plasmajet enthalpy entering the subscale TECS remained nearly constant during the tests. It is important to note that even the uncorrected enthalpy never dropped below 8 MJ/kg, the expected STD/MSPS value.

Thus, there can be no doubt about the severity of the tests to which the TECS components have been subjected so far.

Four important series of tests of the TECS concept were completed. These are:

1. Tests under vacuum conditions, about 400 μm Hg, of vented, complete, subscale TEC systems, which included the MS plus FB plus 1 mil thick aluminum foil MB were performed in the "clean" test facility. Because the force-containment structure around the MB would have increased the complexity and cost of testing, the MB had to be vented (see schematic of Fig. 5). The actual test configuration is shown in Fig. 6. A summary of all these runs is shown in Table III. It is seen that the stagnation enthalpy, static temperature and static pressure of the plasma jet used in these tests exceeded the conditions at the exhaust of the STD/MSPS (*cf.* Table I, p. 2). Table III, along with Fig. 6 also lists the dimensions of the subscale simulators for each run. Typically, these subscale simulators were tested for 15 minutes at 14 MJ/kg initial exhaust enthalpy (pure nitrogen plasma) and at an arcjet stagnation pressure of 1.05 atm. The experimental runs were usually terminated by penetration of the MS and FB. Tests revealed that there was no penetration of the molecular barrier anywhere. However, during a run, the molecular barrier could get hot enough to melt tygon tubing. On the other hand, the gases through the vent were not hot enough to melt plumber's teflon. It was estimated that the energy carried with the gases escaping through the vent and all other losses, *e.g.*, by back radiation to the arcjet housing, was such that, at the worst possible condition, *i.e.*, towards the end of the run, the molecular barrier was radiating the flux corresponding to an exhaust energy flux considerably more than the 8 MJ/kg corresponding to the exhaust flux of the MSPS. Since the surface area of the bag was approximately 17,000 cm^2, the minimum flux of 0.7×10^{-3} kg/s $\times$ 8×10^{6} J/kg = 5.6×10^{3} J/s would correspond to 0.329 W/cm^2, or a black body temperature of about 220°C (493 K), well below the 660°C melting point of aluminum and considerably below the 5.8 W/cm^2 required of a real TECS

device that would be radiating at a black body temperature of about 720°C or 993 K, presumably by use of a nickel foil (melting point 1453°C). Even though the molecular barrier had to be vented for this series of tests, these model experiments were able to prove that all the TECS concept components and energetics work. An important breakthrough of this series of experiments was the observation of a *very uniform* radiation pattern on the filter bag.

2. Tests of the MS and FB in the exhaust of a jet of nitrogen containing Al_2O_3 particles ranging from 1 to 10 μm, centered around 5 μm, were conducted to simulate the STD/MSPS at a total enthalpy of about 13.5 MJ/kg, including all effluents and at an ambient tank pressure of about 0.8 atm. These tests are summarized in Table IV. In one particularly noteworthy run, the unprotected base of the filter bag was penetrated after 3 minutes 52 seconds because a new water-cooled base of the arcjet holder allowed some Al_2O_3 stalagmites to form near the arcjet nozzle, which destabilized the arcjet plume so that it swerved away from the MS target. Because the arcjet was directed away from the MS, the latter was penetrated for less than 40% of its thickness. From this, it can be inferred that the MS would probably have lasted about 10 minutes, even at this high ambient pressure. This test was highly significant because, in the TECS concept, it is the MS that takes the brunt of the attack of the Al_2O_3 particulates in the exhaust. Also, during the same test, there was ample visual proof that the Al_2O_3 in the exhaust was in the form of liquid droplets, stopped mostly at the MS and FB, and that only the finest of the Al_2O_3 slow particles, as judged by their speed, trajectories, and size, made their way past the filter bag.
3. One test of an entire MS plus FB assembly was performed where the pressure in the "clean" vacuum test tank was increased in time from 400 μm Hg to 0.75 atm to simulate some of the actual pressure history effects inside the molecular barrier (Fig. 7). The initial enthalpy of the nitrogen arcjet was 13.8 MJ/kg and the uncorrected final enthalpy was 11.3 MJ/kg. The MS was penetrated after 18 minutes and 45 seconds of high power. This test proved that the gradual pressure rise in the TECS molecular barrier in a continuous run will not present any problems to the MS plus FB assembly. Furthermore, since there is adequate margin of safety for reradiation of the uniformly distributed radiant flux from the FB by the MB, no problems will be presented to the MB. Indeed, the radiation from the FB was remarkably uniform and, if anything, seemed to decrease as the pressure was rising. The decrease was probably caused by switching from the purely radiant heat transfer mode to a partly convective mode at the higher pressures. Since no hot-spot developed on the FB during this transition, no hot spots could have developed on the MB either, as evidenced by the uniform discoloration of teflon tape samples hung at critical locations in the position that would have been occupied by the MB.
4. A test of the concept of the force containment of the molecular barrier was carried out by stretching a foil of 1 mil aluminum across the STD diaphragm tester. This foil was then backed up, on the low pressure side, by carbon fiber woven cloth, made from fibers of thickness 0.05 mm (*cf.* Fig. 8). The measured thickness of the

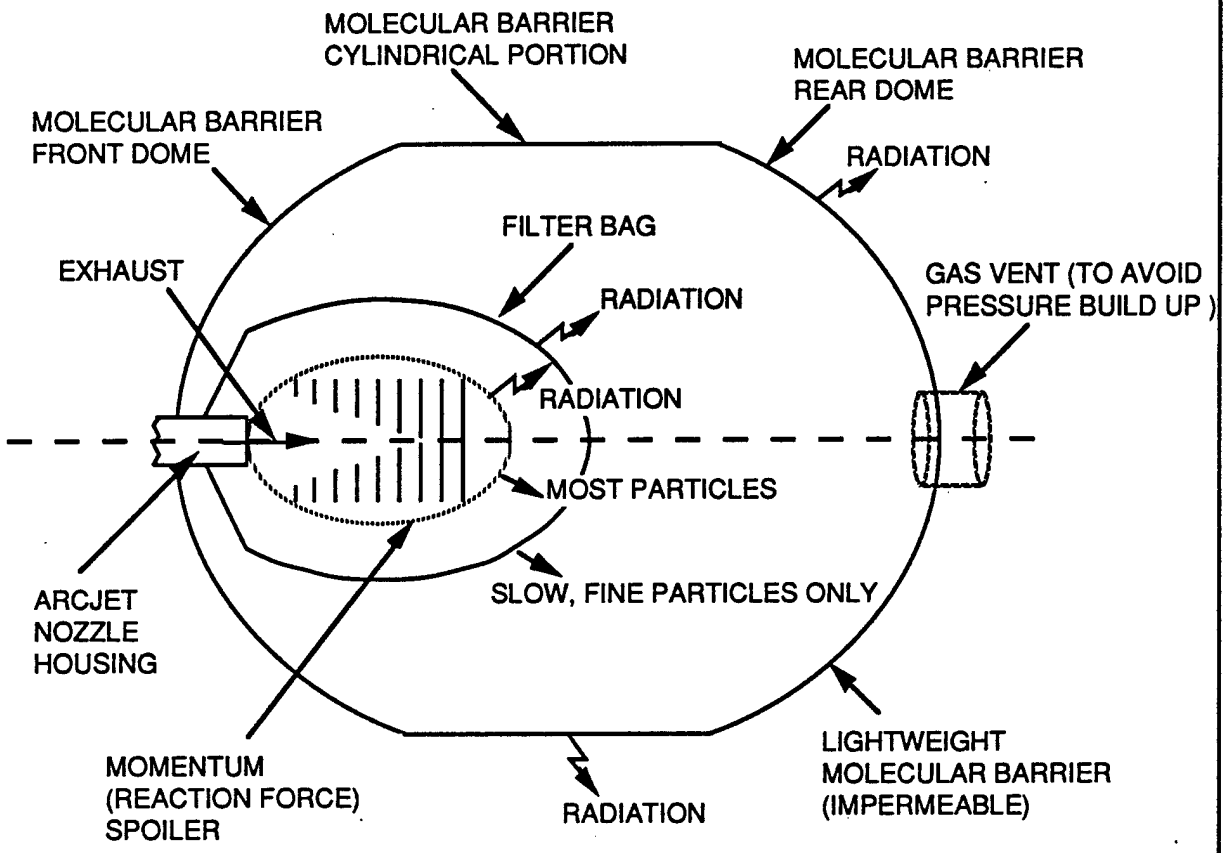

Fig. 5. Schematic of typical TECS subscale simulator configuration for use with the STD Research Corporation High Enthalpy Plasma Flow Facilities (HEPFF). Energy of exhaust is radiated to space from outer bladder which consists of a lightweight molecular barrier and a force containment structure (the latter not shown). Reaction forces are cancelled by the momentum spoiler. Coarse particulates are captured by filter bag. Fine, slow-moving particulates are cooled on the way to molecular barrier and are captured by it. Radiation flux from the molecular barrier to the surroundings cools it and the contained gas. Subscale TECS simulators are allowed to vent gas to avoid pressure build-up since testing with the force containment structure was deemed too expensive at this stage. Venting of the molecular barrier does not affect the physics of the device provided the enthalpy carried off with the escaping gas is a small fraction of total.

9-9051

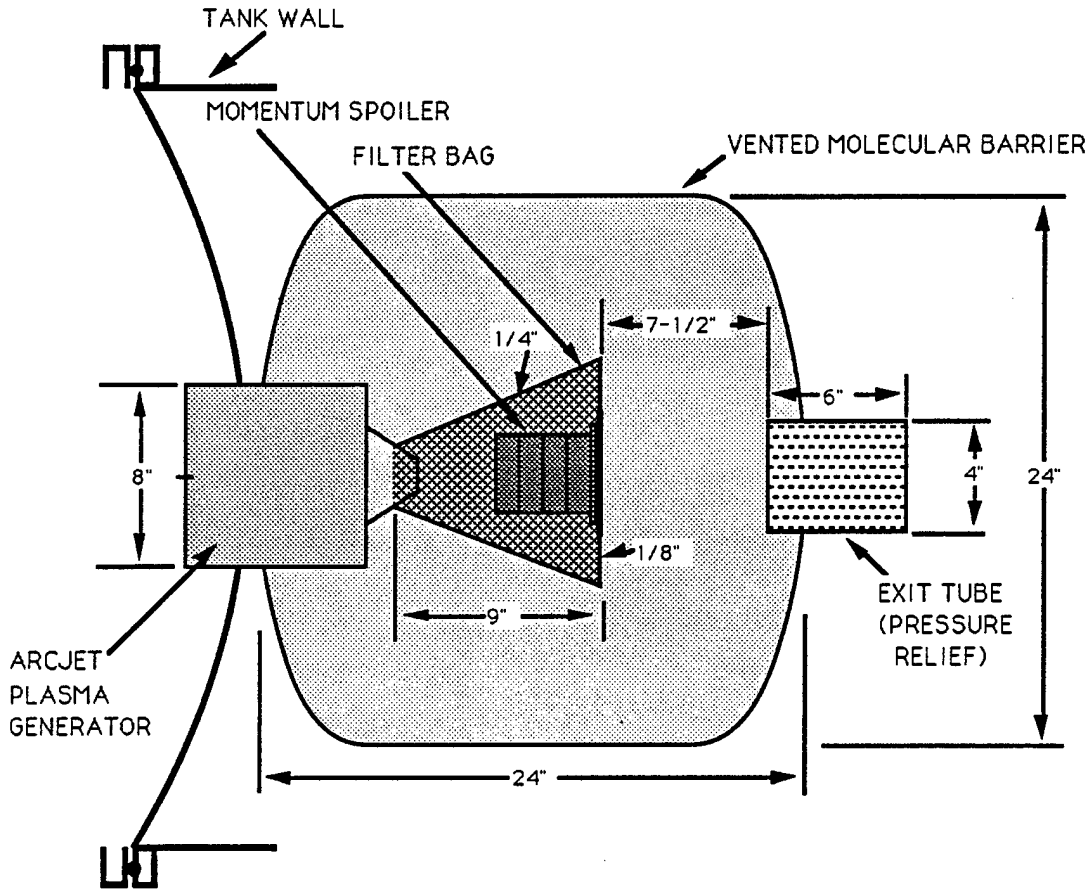

Fig. 6. Dimensions of TECS subscale simulators tested in the STD Research Corporation High Enthalpy Plasma Flow Facilities (HEPFF). Sketch shows most complete TECS subscale simulators; some tests were performed without the filter bag, the vented molecular barrier or both. The length and diameter of the momentum spoiler, the distance between the arcjet and the momentum spoiler and the diameter of the base of the filter bag are listed in Tables III and IV for experiments in the "clean" and "dirty" facilities, respectively. Size of arcjet nozzle exit is 0.55 inch.

8-8020

TABLE III. Summary Of Clean TECS Subscale Tests

Run NO.	MS Diameter (in)	MS Thickness (in)	MS Distance From Arcjet (in)	FB Diameter (in)	MB Diameter (in)	Gas Flow Rate (g/s)	Arcjet Plenum Absolute Pressure (atm)	Enthalpy Range (MJ/kg) High	Enthalpy Range (MJ/kg) Low	Arcjet Exit Velocity (m/s)	Stagnation Temp (K)	Exit Temp (K)	High Power Duration (min)	Pene-tration
1	5.0	0.25	13	not tested	not tested	0.98	1.15	13.3	7.4	3500	6200	4500	14:00	yes
2	5.0	0.25	13	not tested	not tested	0.73	1.08	13.8	9.1	3700	6300	4600	21:40	yes
3	5.0	0.75	13	not tested	not tested	0.75	1.08	14.7	13.9	3900	6400	4700	15:16	no
4	5.0	0.75	13	not tested	not tested	0.73	1.12	17.1	15.1	4300	6500	4800	16:00	no
5a	5.0	0.75	6.5	not tested	not tested	0.76	1.10	16.2	14.7	4200	6300	4600	14:09	yes
5	5.0	1.5	6.6	12.5	not tested	0.73	1.09	14.1	13.8	3800	6400	4700	4:59	no
6	5.0	1.5	6.2	12.5	not tested	0.74	1.12	15.2	13.5	4000	6400	4700	16:00	no
7	5.0	1.0	6.5	12.5	not tested	0.74	1.15	14.4	13.7	3900	6300	4600	16:12	no
8	5.0	1.0	6.5	12.5	not tested	0.74	1.15	14.0	12.6	3800	6200	4500	16:21	no
9	5.0	1.0	6.5	12.5	not tested	0.74	1.15	13.3	13.1	3500	6400	4700	18:15	yes
10	5.0	1.0	6.5	12.5	not tested	0.74	1.02	14.7	12.2	3900	6400	4700	23:40	no
11	5.0	1.0	13	not tested	not tested	0.74	1.02	14.5	12.8	3900	6500	4800	12:40	no
12	3.5	4.0	3.5	11.0	24	0.74	1.02	15.1	14.1	4000	6400	4700	12:19	yes
13	3.5	4.0	3.5	11.0	not tested	0.74	1.02	13.8	11.3	3700	6400	4700	18:45	yes
14	3.5-5.5	4.5	3.3	10.0	24	0.74	1.02	13.6	8.2	3600	6300	4600	14:24	no
15	3.5-5.5	4.5	4.3	11.0	24	0.74	1.00	10.0	9.3	2500	5700	3400	14:56	no
16	3.5-5.0	4.5	3.5	10.0	24	0.74	1.10	11.3	8.6	2900	6000	4500	7:00	no
18	3.5-5.0	4.5	3.5	10.0	24	0.70	0.93	11.8	10.8	3000	6000	4500	8:06	yes

TABLE IV. Summary Of Dirty TECS Subscale Tests

Run NO.	MS Diameter (in)	MS Thickness (in)	MS Distance From Arcjet (in)	FB Diameter (in)	MB Diameter (in)	Total Flow Rate (g/s)	Arcjet Plenum Absolute Pressure (atm)	Enthalpy Range (MJ/kg) High	Enthalpy Range (MJ/kg) Low	Arcjet Exit Velocity (m/s)	Stagnation Temp (K)	Exit Temp (K)	High Power Duration (min)	Pene-tration
A-1	3.5-5.5	6.25	3.5	9.75	not tested	0.96	2.2	15.0	14.0	1700	3800	3500	2:39	no
A-2	3.5-5.5	6.25	3.5	9.75	not tested	0.96	2.2	15.0	14.0	1700	3800	3500	4:54	no
A-3	3.5-5.5	6.25	3.5	9.75	not tested	0.98	2.2	13.8	13.8	1600	3700	3400	3:57	yes
A-4	3.5-5.5	4.5	3.5	10.0	not tested	0.99	2.2	13.5	13.4	1500	3700	3400	3:52	yes
A-5	3.5-5.0	4.5	4.0	10.0	not tested	1.07	2.3	17.9	17.0	1900	3900	3600	5:05	no
A-6	3.5-5.0	4.5	3.5	10.0	not tested	1.08	2.3	29.2	28.4	2600	4300	3700	0:44	yes
A-7	3.5-5.0	4.5	3.5	10.0	not tested	1.08	2.3	13.4	12.7	1500	3900	3400	5:15	yes

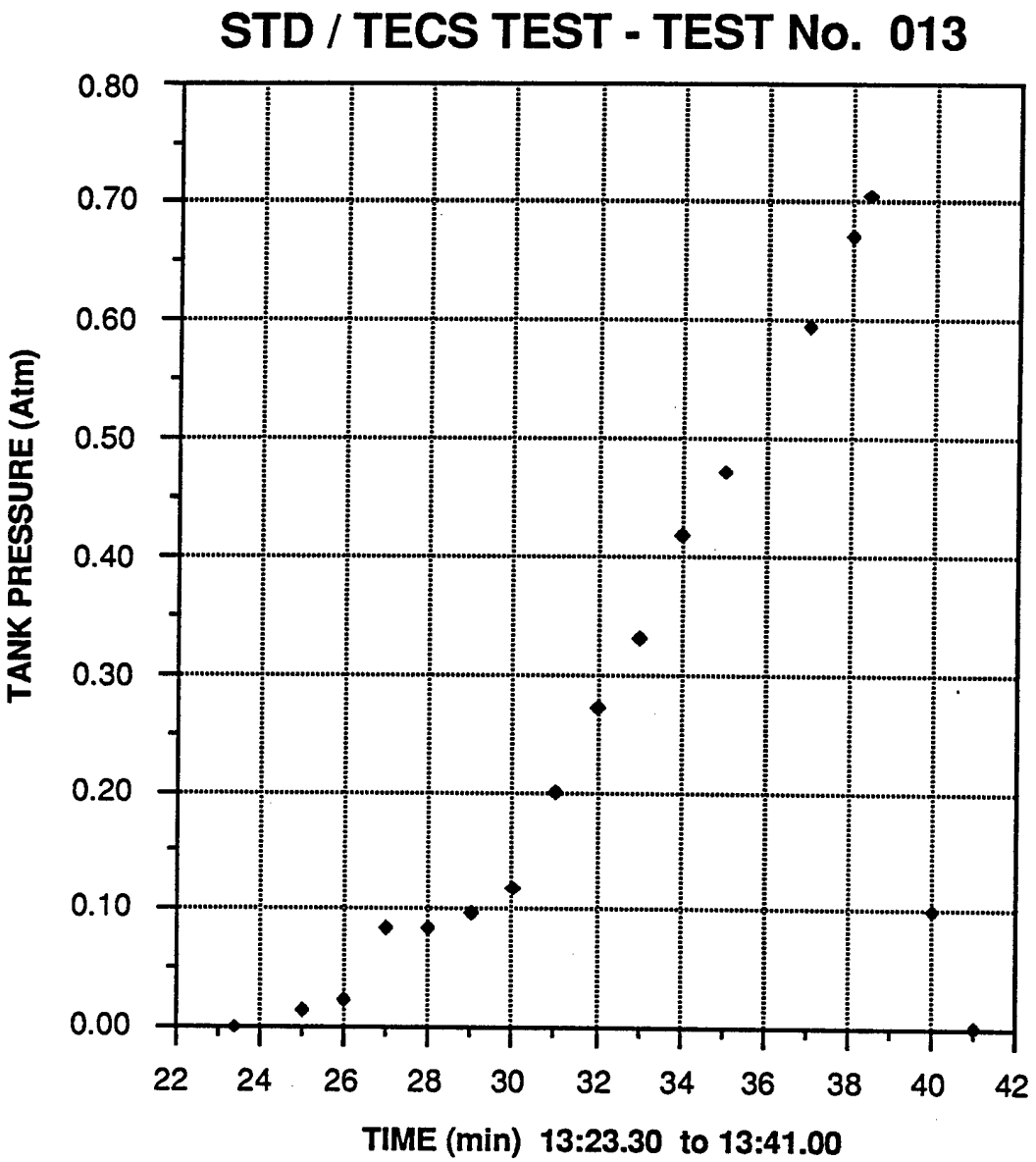

Fig. 7. Pressure in vacuum tank *vs.* time, TECS test no. 13.

8-8925

foil-cloth assembly was 0.15 mm. The carbon fiber cloth weighed 126 g/m^2. This composite "diaphragm" was tested to 200 psi across a 5.5-inch diameter hole before it burst. The permanent deformation of the aluminum foil confirmed that there was some deformation of the composite membrane before it burst. The internal stresses can be obtained from the dome formulas and the strength of the fibers, *i.e.*,

$$S = \frac{pr}{2t_w \sin\theta} = \frac{p}{4t_w}\left(\frac{r^2 + h^2}{h}\right), \tag{44}$$

where S is the internal hoop stress, r is the radius of the diaphragm, θ is the attachment angle of the bulged foil-fiber assembly and h is the height of the bulge (*cf.* Fig. 9). A burst pressure of 150 psi had been predicted from the specifications of the material. The diaphragm burst at a higher pressure than predicted because of failure to allow properly for the elongation and "doming" effect. Nevertheless, this experiment proved that the concept of the force-containment, carbon-fiber structure to support the thin metal foil molecular barrier is mechanically predictable and will work.

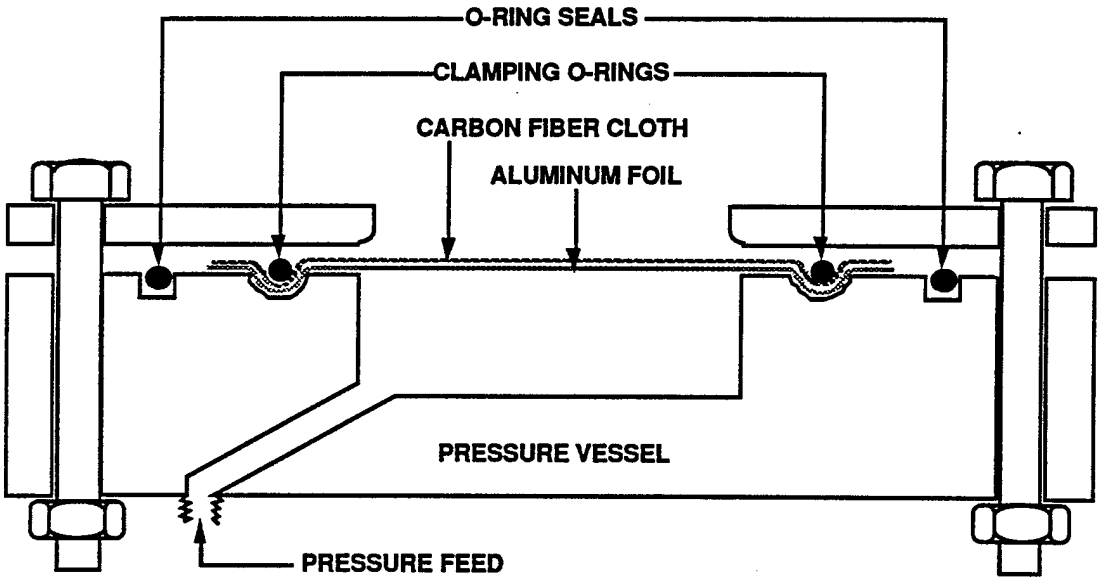

Fig. 8. Schematic of molecular barrier-force containment structure strength test rig.

8-8996

Fig. 10 shows some of the tested TECS components and epitomizes the best achievements of this program to date. Fig. 10a and b show the FB containing the MS under actual test conditions, stopping and uniformly reradiating the energy from a

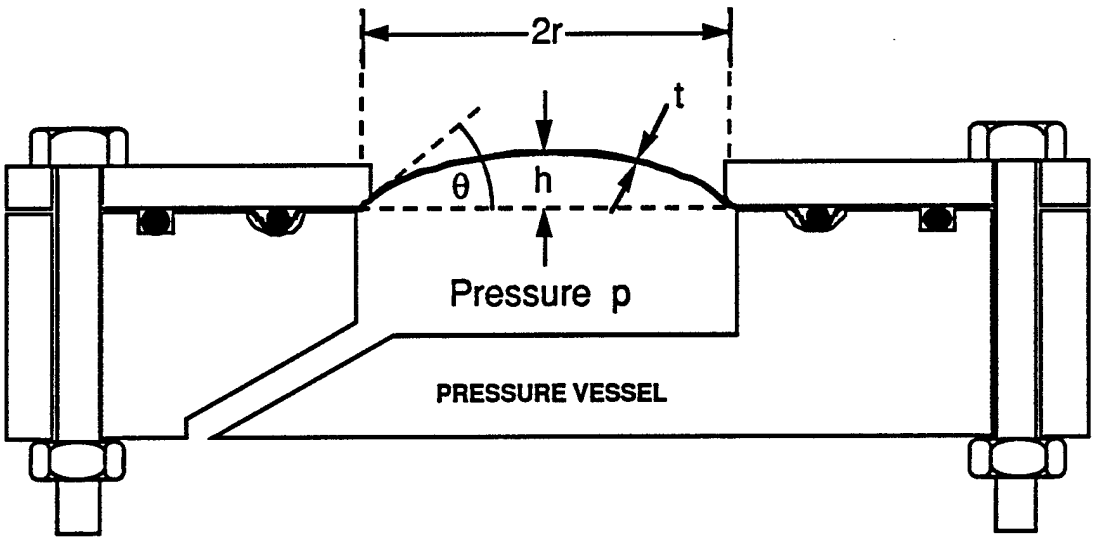

Fig. 9. Schematic of molecular barrier-force containment structure strength test rig; nomenclature.

8-9166

nitrogen plasmajet at 13 to 15 MJ in the clean test tank. Fig. 10c and d show the pre-test and post-test condition of an entire TECS assembly (MS plus FB plus vented MB). The MB consisted of 1 mil thick aluminum foil. It was vented in order to avoid surrounding it with the expensive carbon fiber force-containment structure. Care was taken to minimize enthalpy losses by the gas escaping from the vent and by radiation to the arcjet housing.

3. SUBTASK 2.3: FINAL CONCEPTUAL DESIGN AND FEASIBILITY ASSESSMENT

The objectives of this subtask were to carry out a final conceptual design and assess the feasibility of the proposed TEC system, to identify any remaining technical uncertainties and make recommendations for their resolution in larger-scale ground tests.

On the basis of the mass of the components used in experiments with the TECS subscale simulators and their interpretation through the models and scaling analyses presented above, it is possible to arrive at a good estimate of the total mass of a TEC system applicable to the STD/MSPS. Therefore, the final conceptual design is obtained by combining the results from the analytical study of Task 1 with the experimental investigation of Task 2. The size and mass of the momentum spoiler and filter bag are obtained from the scaling laws and the experimental results. The mass for the molecular barrier/force containment structure assembly is evaluated using the purely radiative heat transfer model. It is found that the total mass of the TECS system relevant to the STD/MSPS is projected to be around 6000 kg or 25% of the fuel plus oxidant mass, if there is no diffusion allowed through the molecular barrier.

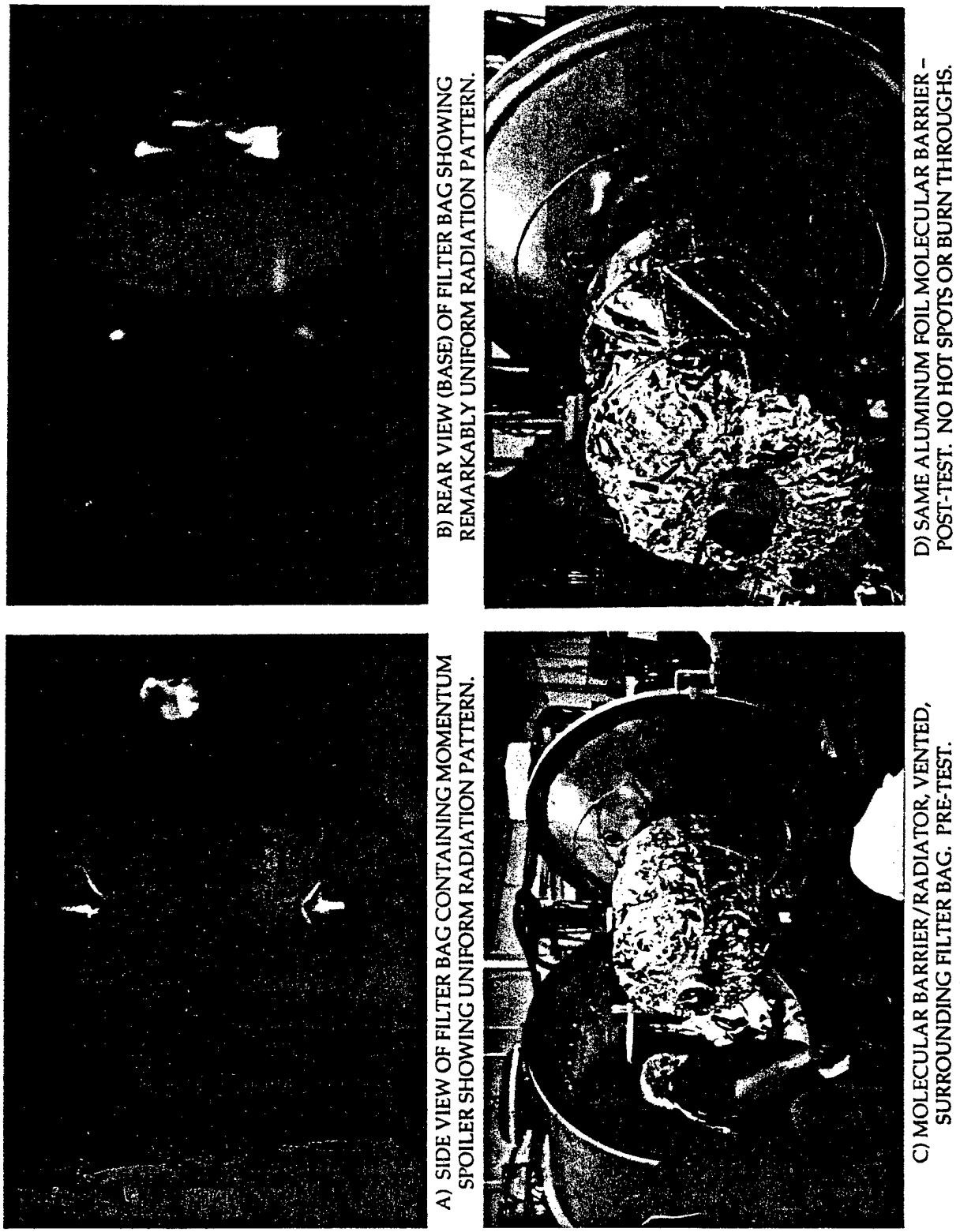

Fig. 10. Highlights of TECS experiments at the Plasma Flow Facility in the STD Research Corporation Laboratory.

3.1 Momentum/Energy Spoiler

The proposed MS for the TECS applicable to the STD/MSPS, shown in Fig. 11, is designed mostly from experience with subscale TECS testing. It was found that a layer of carbon felt material having a thickness of 15 cm could sustain a plasma exceeding the requirements of the MSPS for more than the required 500 seconds. Furthermore, it was found that the diameter of the active portion of the MS has to be about twice that of the plasma jet. To spoil the momentum and energy of the greatly underexpanded MSPS at the start of a run when the bag pressure is almost negligible, the MS completely encloses the plasma jet with layers of varying thickness. The entire assembly is supported by carbon rods which transmit most of the reaction forces back to the MSPS. The mass of the MS is estimated at 690 kg and that of the carbon rods at 130 kg.

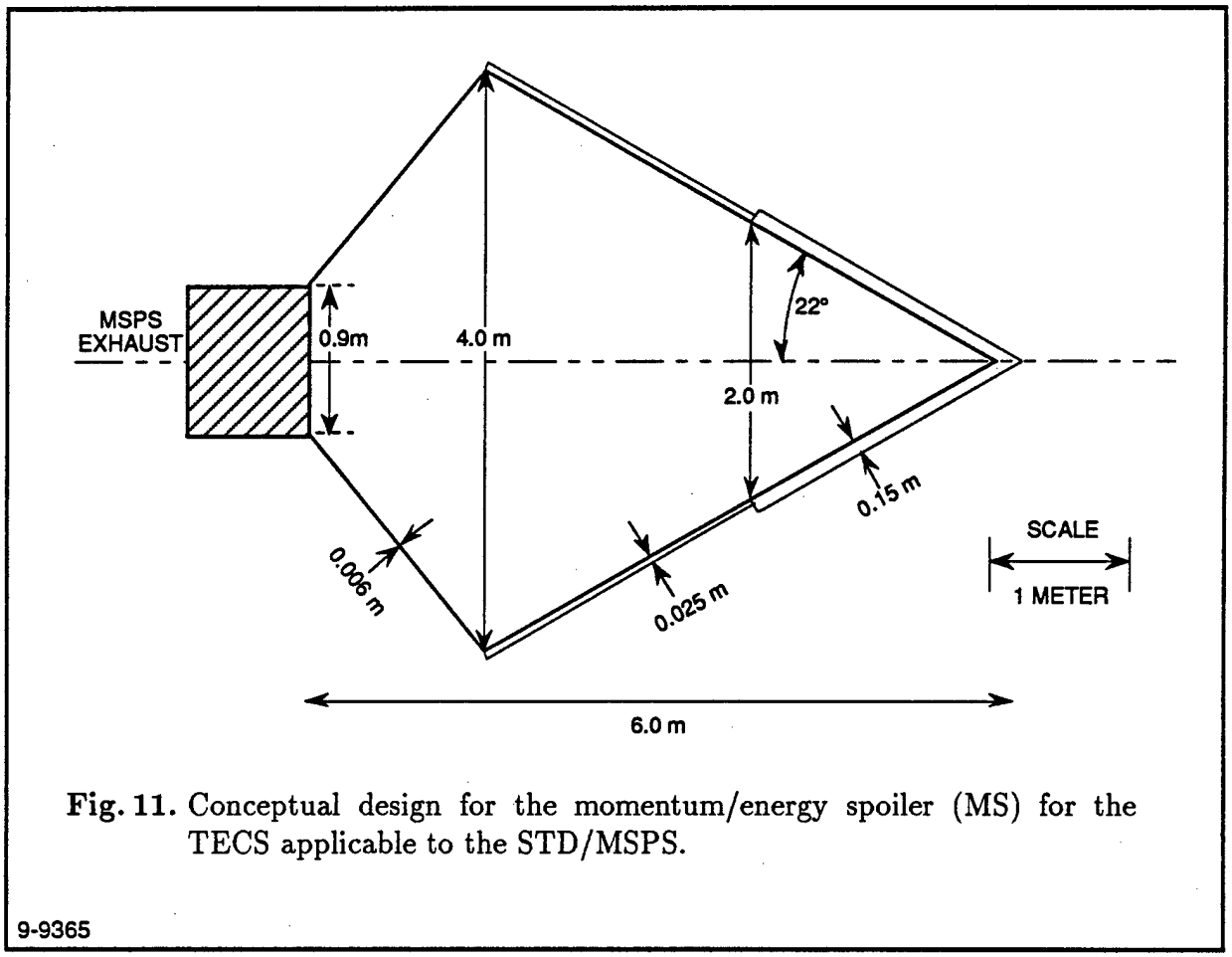

Fig. 11. Conceptual design for the momentum/energy spoiler (MS) for the TECS applicable to the STD/MSPS.

3.2 Filter Bag

The proposed FB for the TECS applicable to the STD/MSPS is chosen to be spherical instead of conical as was used for the subscale experiments. The conical design was chosen for the experiments only for its ease of manufacture. The spherical design offers a more uniform radiation pattern and does not require structural components to

preserve its shape. The scaling laws, as well as the experimental results, are used to obtain a conceptual design for the FB comprising a 15.1 m diameter sphere, 6 mm thick, having a mass of 390 kg. Although experiments have shown that the filter bag is very porous and lets particles smaller than about 5 μm through (which includes most of the particles since they are in the 1–3 μm range (*cf.* Ref. 1)), possible pressure build up requires that the FB be supported by a force containment structure similar to that of the molecular barrier. A conservative estimate for its equivalent thickness and mass are 0.2 mm and 240 kg, respectively. It should be noted that adding such a thin layer of carbon fiber, possibly configured as a net, will not alter significantly the filtering properties of the FB. Therefore, the mass of the complete filter bag assembly is estimated at 630 kg.

3.3 Molecular Barrier and Force Containment Structure

Nickel is selected as the molecular barrier material since it has a much higher melting temperature (1726 K) than aluminum (993 K). The molecular barrier is proposed to be 8×10^{-3} mm thick, as a trade-off between minimal mass and low porosity. Using the optimization approach outlined in Section 3, Chapter II, with an emissivity of the bag material of $\epsilon = 0.9$, the bag radius is chosen to be 35 meters. From this, the mass of the molecular barrier is estimated at 1100 kg and that of the force containment structure at 3700 kg, for a total of 4800 kg.

It should be noted that if nickel is replaced as the molecular barrier material by aluminum at the same thickness, the optimum bag radius is increased to 53 m and the total mass of the molecular barrier/force containment structure assembly is reduced to 3800 kg. Furthermore, since the bag radius is increased, its surface temperature is decreased to about 700 K, which is low enough for use with aluminum.

The preferred method for the manufacture of the force containment structure is to weave a one-piece spherical structure. However, this method appears to be very expensive. Another method is to manufacture the bag assembly from pieces of carbon fiber cloth and metal foil sewn together into a spherical structure. There are companies that specialize in the stitching of such large assemblies, which is performed with rail mounted industrial stitching heads. For example, Saltech Inc. of Montreal, Canada, assembled the roof of the Montreal Olympic stadium, which is made from 1 mm-thick rubber coated Kevlar cloth. To ensure proper sealing and structural integrity at the seam, an overlapping lockstitch is recommended (Fig. 12); since the carbon fiber cloth is thin, the bending stresses at the folds are reduced by using a thin carbon cable.

3.4 Summary

A sketch of the TECS applicable to the STD/MSPS is shown in Fig. 13. The estimated temperature of each component, as well as that of the effluents in-between, is shown in Fig. 14.

Table V shows the mass breakdown by component; the total, 6,250 kg, is 25% of the fuel plus oxidant mass for the STD/MSPS and is the best current estimate. It should be noted that this estimate is probably conservative since subscale test enthalpies for the MS and FB were 20% to 50% higher and the test times to penetration 50% to 100% longer

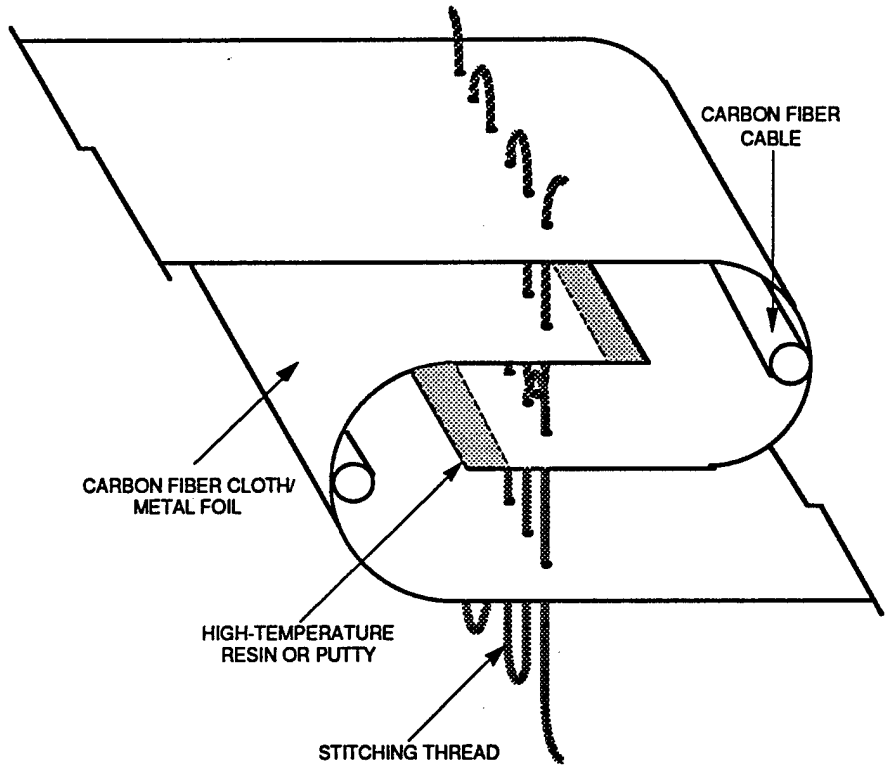

Fig. 12. Schematic of possible seam for fabricated molecular barrier/force containment structure assembly. In case it has to be sewn it may look as shown on this diagram. However, the completely woven one-piece assembly is preferred.

9-9380

than for the STD/MSPS. There is therefore a built-in safety factor in the current estimate. Also, if aluminum is used in place of nickel as the molecular barrier material, the mass of the TECS is reduced to 5,250 kg, or 21% of the fuel plus oxidant mass for the STD/MSPS.

Also shown in Table V are cost estimates of materials for the construction of a full-size TECS relevant to the STD/MSPS. The total cost of materials is estimated to be about $900,000. We estimate that the labor cost to perform the assembly of the full system to be another $900,000, for an estimated total cost of $1,800,000 per unit. It should be noted that if the TECS system is built with the aluminum molecular barrier at a mass saving of 1000 kg, the estimated cost for the materials and labor for this complete TECS assembly is increased to $3,700,000. The increase in cost with respect to the device using a nickel foil is mainly due to the large size of the bag assembly of the aluminum device.

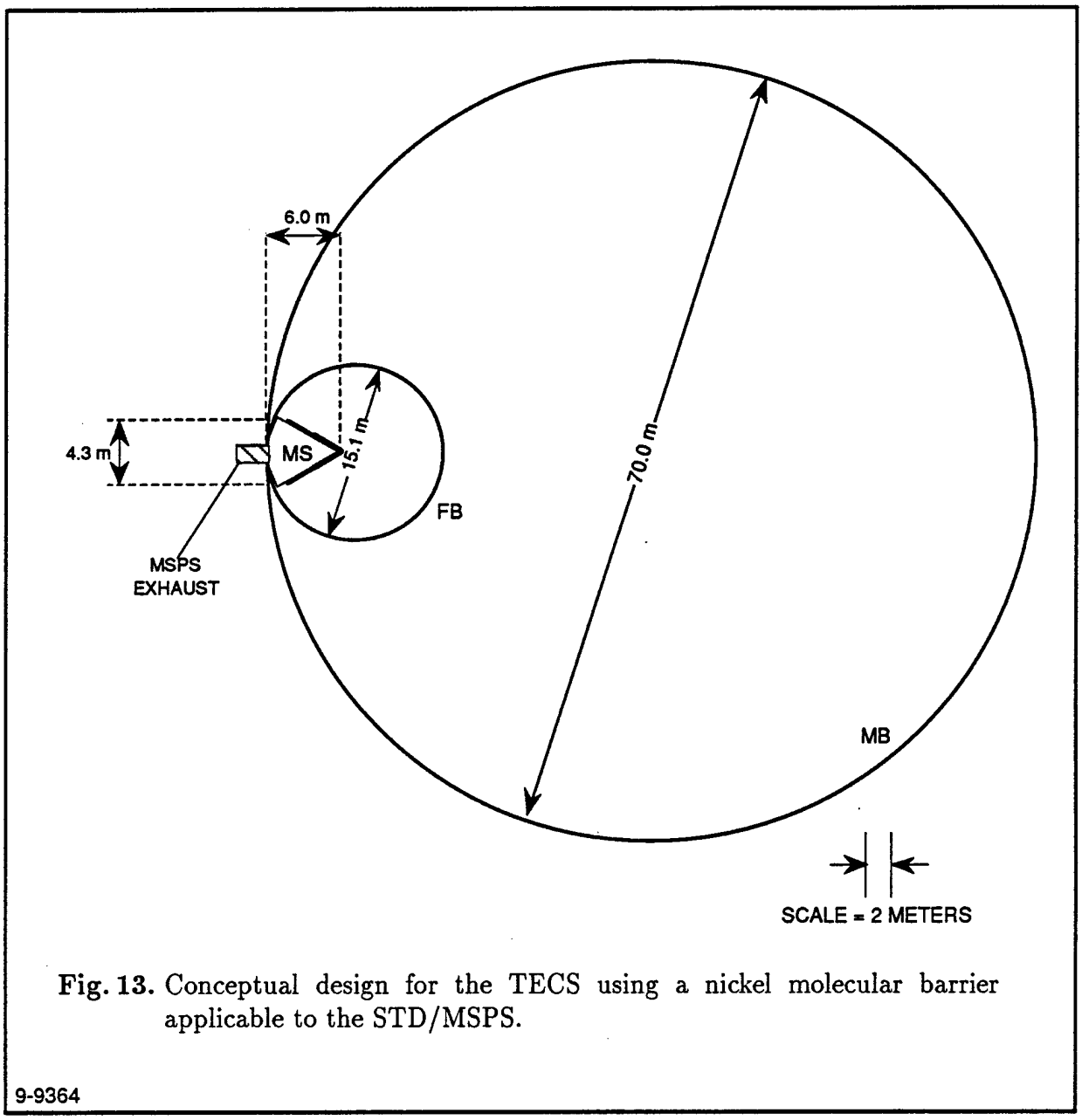

Fig. 13. Conceptual design for the TECS using a nickel molecular barrier applicable to the STD/MSPS.

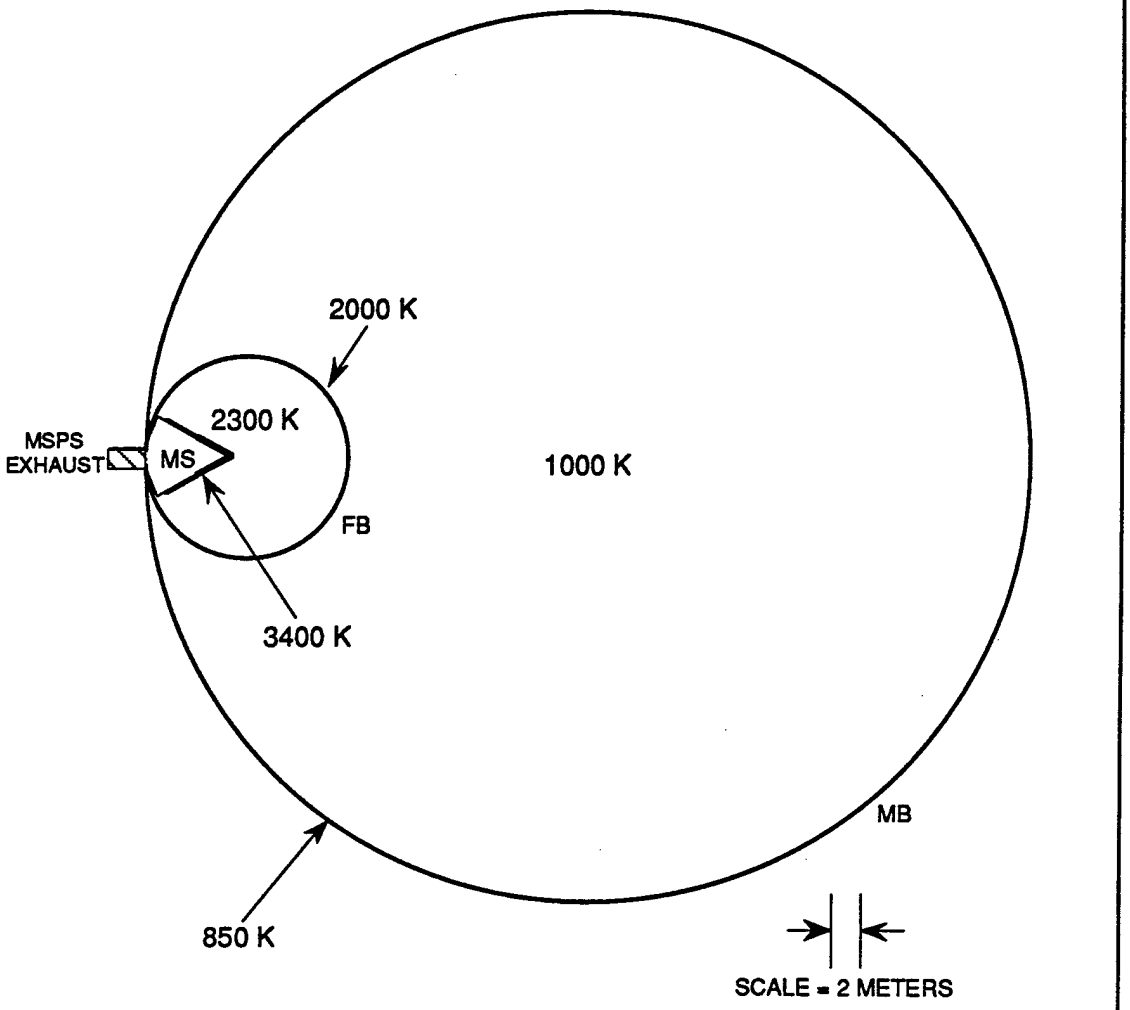

Fig. 14. Temperature distribution for conceptual design of TECS using a nickel molecular barrier applicable to STD/MSPS. Temperatures are evaluated using a stricly radiative heat transfer model (*cf.* Chapter II, Section 1.1.3.2).

Table V. Best Estimate of Mass and Material Cost of TECS Components for 100 MW_e/500 s Continuous Burst MSPS

Component	Mass (kg)	Cost
Momentum spoiler	690	$64,000
Support structure	130	$10,000
Filter bag	390	$36,000
FB Force containment structure	240	$34,000
Molecular barrier (Nickel)	1100	$21,000
MB Force containment structure	3700	$738,000
Total	6,250 kg	$903,000

CHAPTER IV

CONCLUSIONS

STD Research Corporation has demonstrated, on a laboratory scale, the feasibility of exhaust effluent and reaction force containment for a family of open-cycle space power systems in general and the STD MHD Space Power System in particular. The advent of new materials and new technologies has made it possible to devise an affordable and promising concept for the control of open-cycle exhaust products and reaction forces, and the suppression or elimination of their harmful influences.

In part under DOE/PETC Contract DE-AC-22-87PC79677, STD Research Corporation has performed computations and developed subscale laboratory simulators to demonstrate the feasibility of a Total Exhaust Containment Systems (TECS) concept of wide applicability. It investigated methodologies and conceptual designs for improving the performance and establishing the engineering data base for this concept, with special emphasis on mass reduction and life improvement of the TECS. It calculated and simulated the TECS performance with the appropriate restricted STD Research computer codes and was able to choose the most promising concept. It conducted intensive laboratory tests to determine the most suitable materials for each TECS component and carried out critical experiments in the STD Research high-enthalpy Plasma Flow Facility to validate the calculated results. It evaluated the mass of a TEC system relevant to the STD/MSPS and found that such a system would represent approximately 21% to 25% of the fuel plus oxidant mass for a pulse of 100 MW_e over 500 seconds.

It is also clear from this work that TEC systems of even lower mass and improved specifications, characteristics and performance can be designed and built if additional effort is put into this project. Selection of an appropriate solution to the problem of meteoroid and space debris punctures and/or damage must be initiated. Additional work is required to reduce the temperature of the STD/MSPS exhaust and the final temperature of the gases inside the molecular barrier (MB) bag even further, to increase the emissivity of the MB, to reduce the mass of the MB and its force-containment structure, and to find MB materials that permit harmless effluents such as hydrogen and perhaps nitrogen and some other gases to escape or leak from the MB while the harmful particulates and gases remain inside. A reduction of the mass of a space-hardened TEC system by a factor of two appears feasible.

Also, one must not lose sight of the fact that advances in materials science research will lead to fibers of even greater strength. That and improvements in the enthalpy extraction of the MSPS system, perhaps by a cogeneration or combined-cycle system

approach, will bring about a dramatic reduction of the TECS mass, since a large fraction of it is taken by the force containment structure of the molecular barrier. Additional work is required to improve the accuracy of all the measurements and diagnostics, for example by measuring the temperature distribution of the filter bag and molecular barrier, and the realism of the subscale model simulator tests by building a *complete* TECS subscale simulator, including the force containment structure, and firing a small subscale hybrid rocket motor into it. Finally, the analytical models have to be improved, by performing a full spectral radiative heat transfer calculation including conduction and convection effects, to refine the weight estimate. These improvements were proposed by STD Research Corporation in Proposal STD-SP-006-89 of 31 March 1989 in response to PRDA DE-RA22-89PC89799.

On the basis of the theoretical and experimental results presented in the original proposal by STD Research Corporation of 27 January 1987 in response to the DOE/PETC Proposal Request PRDA RA22-87PC90271 and the experimental results obtained after the award of Contract DE-AC22-87PC79677 (start date 14 September 1987) and independently validated and verified by the junior authors of this report by repeating the theoretical analyses of Chapter II and some of the experiments described in Chapter III, namely tests No. 18 and A-7, in order to check the results and obtain additional data during the course of this investigation, it is concluded that the TECS concept proposed by STD Research Corporation exceeds the effluent control requirements for magnetohydrodynamic space power systems set forth on page 34 of the National Research Council Report entitled "Advanced Power Sources for Space Missions, 1989" (Library of Congress Catalog Card No. 88-63907).

References

1. Hoglund, R.F., "Recent Advances in Gas-Particle Nozzle Flows," *ARS Journal,* May 1962, p. 662–671.
2. Kreith, F. and Black, W.Z., "Basic Heat Transfer," Harper and Row, New York, 1980, p. 346–357.
3. Rohsenow, W.M. and Hartnett, J.P., editors, "Handbook of Heat Transfer," McGraw-Hill, New York, 1973, p. 15-29.

Appendix

Composition of STD/MSPS effluents at two typical conditions. Condition 1 is typical of effluents issuing from the MHD generator, *i.e.*, at the entrance of the TECS. Static temperature and pressure are 3200 K and 0.39 atm, respectively. Condition 2 is typical of effluents within the TECS system. Static temperature and pressure are 900 K and 0.27 atm, respectively. Species accounting for less than 0.1% by mole fraction are not listed.

Species	Mole Fraction at Condition 1 (%)	Mole Fraction at Condition 2 (%)
Al	0.4	—
AlO	0.5	—
AlOH	0.1	—
AlO_2H	0.1	—
$Al_2O_{3(\ell)}$	17.5	—
$Al_2O_{3(s)}$	—	20.6
$C_{(s)}$	—	3.2
CH_4	—	0.3
CO	28.9	21.6
CO_2	1.6	9.4
Cs	0.7	—
Cs^+	0.2	—
CsOH	—	0.8
$Cs_2(OH)_2$	—	0.1
e^-	0.1	—
H	12.2	—
H_2	7.6	16.2
H_2O	3.2	3.0
NO	0.4	—
N_2	21.7	24.8
O	2.0	—
OH	2.0	—
O_2	0.3	—
	99.5	100.0